



Mechanisms of biostimulant-enhanced biodegradation of PAHs and BTEX mixed contaminants in soil by native microbial consortium

Mukhtiar Ali ^{a,b}, Xin Song ^{a,b,*}, Qing Wang ^a, Zhuanxia Zhang ^{a,b}, Jilu Che ^a, Xing Chen ^c, Zhiwen Tang ^{a,b}, Xin Liu ^a

^a Key Laboratory of Soil Environment and Pollution Remediation, Institute of Soil Science, Chinese Academy of Sciences, Nanjing, 210008, China

^b University of Chinese Academy of Sciences, Beijing, 100049, China

^c China Construction 8th Engineering Division Corp., LTD, Shanghai, 200122, China



ARTICLE INFO

Keywords:

Co-contamination
Biostimulation
Bioavailability
Enzymes
Microbial consortium
Microbial metabolisms

ABSTRACT

Despite the co-occurrence of polycyclic aromatic hydrocarbons (PAHs) and benzene, toluene, ethylbenzene, and xylene (BTEX) in the field, to date, knowledge on the bioremediation of benzene and benzo[a]pyrene (BaP) mixed contaminants is limited. In this study, the mechanisms underlying the biodegradation of benzene and BaP under individual and co-contaminated conditions followed by the enhanced biodegradation using methanol, ethanol, and vegetable oil as biostimulants were investigated. The results demonstrated that the benzene biodegradation was highly reduced under the co-contaminated condition compared to the individual benzene contamination, whereas the BaP biodegradation was slightly enhanced with the co-contamination of benzene. Moreover, biostimulation significantly improved the biodegradation of both contaminants under co-contaminated conditions. A trend of significant reduction in the bioavailable BaP contents was observed in all biostimulant-enhanced groups, implying that the bioavailable BaP was the preferred biodegradable BaP fraction. Furthermore, the enzymatic activity analysis revealed a significant increase in lipase and dehydrogenase (DHA) activities, as well as a reduction in the catalase and polyphenol oxidase, suggesting that the increased hydrolysis of fats and proton transfer, as well as the reduced oxidative stress, contributed to the enhanced benzene and BaP biodegradation in the vegetable oil treatment. In addition, the microbial composition analysis results demonstrated that the enriched functional genera contributed to the increased biodegradation efficiency, and the functional genera in the microbial consortium responded differently to different biostimulants, and competitive growth was observed in the biostimulant-enhanced treatments. In addition, the enrichment of *Pseudomonas* and *Rhodococcus* species was noticed during the biostimulation of benzene and BaP co-contamination soil, and was positively correlated with the DHA enzyme activities, indicating that these species encode DHA genes which contributed to the higher biodegradation. In conclusion, multiple lines of evidence were provided to shed light on the mechanisms of biostimulant-enhanced biodegradation of PAHs and BTEX co-contamination with native microbial consortiums.

1. Introduction

Polycyclic aromatic hydrocarbons (PAHs) and BTEX (benzene, toluene, ethylbenzene, and xylene) are organic compounds that have long been known as hazardous to threaten human health. Benzo[a]

pyrene (BaP) and benzene, among all PAHs and BTEX, are the most commonly detected and toxic to human health (ATSDR, 2019). They have been widely spread due to anthropogenic activities at gas stations, steel-making factories, the coal chemical industry, and rural tunnels (traffic-related emissions) (Chen et al., 2018; Dobaradaran et al., 2021;

Abbreviations: PAHs, Polycyclic aromatic hydrocarbons; BTEX, Benzene, Toluene, Ethylbenzene and Xylene; BaP, Benzo[a]pyrene; ATSDR, Agency of Toxic Substances and Disease Registry; DHA, Dehydrogenase; LIP, Lipase; CAT, Catalase; PPO, Polyphenol oxidase; HPLC, High-Performance Liquid Chromatography; GC-MS, Gas Chromatography coupled Mass Spectrometry; CK-1, Control with no contamination; CK-2, Biocide control ($HgCl_2$); BS-ethanol, Biostimulation with ethanol; BS-methanol, Biostimulation with methanol; BS-VO, Biostimulation with vegetable oil.

* Corresponding author. Key Laboratory of Soil Environment and Pollution Remediation, Institute of Soil Science, Chinese Academy of Sciences, Nanjing, 210008, China.

E-mail address: xsong@issas.ac.cn (X. Song).

<https://doi.org/10.1016/j.envpol.2022.120831>

Received 27 June 2022; Received in revised form 29 November 2022; Accepted 4 December 2022

Available online 9 December 2022

0269-7491/© 2022 Elsevier Ltd. All rights reserved.

Gaga et al., 2018; Liu et al., 2019b; Williams & Khodier, 2020). Benzene and BaP can co-exist due to petroleum oil exploitation, smelting operations, and thermal activities (Baranger et al., 2021; Chen et al., 2018; Muller et al., 2017), resulting in their co-contamination in soil. Both BaP and benzene have low water solubilities and can persist in soil in non-aqueous-phase liquids (NAPLs), tar, or solid particles (Russold et al., 2006; Lominchar et al., 2018; Perini et al., 2020; Sharma et al., 2020). Due to the detections of mixed contamination in the soil, as well as their high carcinogenicity and teratogenicity, there is an urgent need for the remediation of these mixed contaminants.

Bioremediation is the use of microorganisms to remediate contaminants from different environmental media (Subashchandrabose et al., 2019; Wu et al., 2019), which is a cost-effective and eco-friendly remediation approach for xenobiotics, including BaP and benzene from the environment (Baranger et al., 2021; Zegzouti et al., 2020). However, the lack of easily degradable substrates reduces microbial activities, thereby resulting in slow degradation (Paneque et al., 2020; Rodriguez-Morgado et al., 2015; Zeng et al., 2021). Therefore, substrates in the form of carbon/nutrients have been applied to enhance the bioremediation capability of microorganisms. The addition of substrates to the contaminated site, known as biostimulation (Ali et al., 2022; Paneque et al., 2020), can promote microbial and enzymatic activities under high contamination conditions by acting as the energy-providing metabolite and reducing the concentration of hazardous contaminants (Liu et al., 2019a; Zhao et al., 2019). Several biostimulants, including vegetable oil (Borden, 2007; Kao et al., 2016; Pfeiffer et al., 2005), ethanol (Cardenas et al., 2008; Song et al., 2021), and methanol (Zhao et al., 2019; Zhao et al., 2018), have been used to enhance the biodegradation of different contaminants.

Numerous studies reported the biostimulant-enhanced biodegradation of benzene under both aerobic conditions (e.g., Nicholson & Fathepure, 2004; Yang et al., 2019) and anaerobic conditions using carbon, nitrate, sulfate, or iron as electron acceptors (Xiong et al., 2012; Muller et al., 2017; Xiong et al., 2017) (Table S1). Biostimulation has been reported to have an inhibitory or stimulatory effect on microbial diversities (Fu et al., 2021; Wu et al., 2017). For example (Fu et al., 2021), reported that biostimulation can cause a reduction in diversity indices (Fu et al., 2021). On the other hand, high concentrations of contaminants create a toxic influence on microorganisms; therefore, biostimulation of these contaminated soils has no effect on bacterial indices (Song et al., 2021; Wu et al., 2019). Moreover, carbon-enriched biostimulants can act as a rich source of energy, enhancing microbial richness and diversity under different contaminated conditions (Song et al., 2021; Wu et al., 2017). Therefore, it is essential to explore the carbon-enriched biostimulants for the biodegradation of benzene and BaP co-contaminated soil, and their consequent influence on microbial structure and diversity.

Despite the co-occurrence of PAHs contaminants and BTEX in the field (Baranger et al., 2021; Ali et al., 2022; Muller et al., 2017), to date, knowledge of the biodegradation of benzene and BaP mixed contaminants and the mechanisms of their influence on bioremediation are limited. Therefore, considering the importance of biostimulation and the hazardous impact of benzene and BaP co-contamination, a series of microcosm experiments were conducted using different biostimulants to determine (1) the impact of BaP and benzene co-contamination on bioremediation, (2) the enzymatic activities in BaP and benzene co-contaminated soils under biostimulation, and (3) the microbial community compositions and abundance under benzene and BaP co-contamination conditions.

2. Materials and methods

2.1. Chemicals and reagents

Standard solutions of Σ16 PAHs, BaP, and benzene were purchased from Sigma-Aldrich (St. Louis, MO, USA). Acetonitrile (99.9% pure) and

n-hexane (95% pure) were supplied by Merck (Darmstadt, Germany). Dichloromethane (99.8%) and n-butanol (99%) were obtained from Aladdin Bio-Chem Technology Co. Ltd. (Shanghai, China). All the chemicals used in this experiment were of analytical high-performance liquid chromatography (HPLC) grade.

2.2. Soil sampling and preparation

The soil was collected from the BD-1458 site of a steel-making factory (Hangzhou, Zhejiang Province, China) at a depth of 1–2 m and air-dried at room temperature. The air-dried sieved soil was analyzed for its physical, chemical, and biological properties, including the concentrations of Σ15 PAHs (Table S3). Despite the inclusion of 16 PAHs priority pollutants, owing to detector constraints of HPLC, acenaphthylene was not detected during the analysis. Therefore, Σ15 PAHs were analyzed during the experiment. The average concentration of BaP and benzene in the steel-making factory site is 50 mg kg⁻¹ each. However, the collected soil contained 5.316 mg Σ15 PAHs kg⁻¹, and the BaP concentration was lower than the contamination level of 50 mg kg⁻¹. Also, none of the benzene was detected in the collected soil samples. Therefore, the soil was artificially spiked with BaP and benzene to reach the maximum contamination level of 50 mg BaP kg⁻¹ soil and 50 mg benzene kg⁻¹ soil, respectively, as described below.

2.3. Soil spiking

Artificial contamination was accomplished for both contaminants, and 4 kg of soil was first spiked with 50 mg BaP kg⁻¹ according to the procedure described previously (Picariello et al., 2020). Briefly, 2000 mg L⁻¹ standard solution was prepared by dissolving 0.2 g of BaP in 40 mL of acetone. Then, the standard solution was spiked with 320 g of soil and mixed thoroughly, and the mixture was left overnight to evaporate the acetone in fume-hood. Subsequently, the contaminated soil was mixed with the remaining 3.6 kg of clean soil to obtain the final concentration of 50 mg BaP kg⁻¹ soil. Six random samples were collected and analyzed for BaP concentration, which was found to be 48 ± 0.02 mg kg⁻¹. The soil was kept in dark for three months to allow the interaction of BaP with soil particles for aging prior to the experiment. Similarly, benzene artificial contamination was done after the completion of the aging time for BaP. A 600 mg L⁻¹ standard benzene solution was prepared using acetone as solvent. Then, a small amount of 600 mg L⁻¹ standard solution was spiked with a known quantity of BaP-contaminated soil to obtain 50 mg benzene kg⁻¹ soil as the final concentration. The ratio of acetone and soil was selected in such a way that the native microorganisms were less disturbed. The solution and soil were gently mixed to equally distribute benzene and BaP throughout the soil. Due to benzene volatilization, the soil was not kept for aging, and the experiment was started directly after spiking the BaP-contaminated soil with benzene.

2.4. Experimental setup

The BaP-benzene contaminants spiked soil (120 g) was placed in 250-mL identical bottles and sealed aseptically with blue rubber septa and aluminum crimp covers. Prior to the benzene and BaP co-contaminated experiment, a pre-experiment was conducted to find out the biodegradation of individual and co-contamination of BaP and benzene. The results have been explained in the supplementary file (Section 3.1). In addition, a pre-experiment to evaluate the loss of BaP due to the use of acetone as a solvent for BaP, which is a practice often used for the preparation of artificially contaminated soil (Brinch et al., 2002; Picariello et al., 2020; Olivito et al., 2021; Muller et al., 2022). It was found the butanol-extractable BaP was 38.9 ± 1.2 mg kg⁻¹ in soils without the addition of acetone after the three months of aging time. However, the butanol extractable BaP was 43.4 ± 1.7 mg kg⁻¹ with the addition of acetone. This indicated that the addition of acetone

increased the butanol-extractable BaP by causing the desorption of BaP from soil samples (Qin et al., 2020). For the co-contamination experiment, different biostimulants including, ethanol, methanol, and vegetable oil were used to enhance microbial activity, enzyme regulation, and bioremediation of the co-contaminants, and were added directly after the benzene spiking. Previous studies reported that these biostimulants (ethanol, methanol, and vegetable oil) can be used by microorganisms as a preferential carbon source to enhance the biodegrading capabilities of microorganisms (Table S2). The vegetable oil (VO) used in this study was a byproduct from a factory producing vegetable fat (recycled wasted vegetables) using plants such as beans and palm trees, and the concentrations of different elements were measured in VO (Table S3). A solution consisting of 300 mM ethanol and methanol was prepared using sterile ultrapure milli-Q water and 40 mL of the solution was added to the specified bottles to get the final 100 mM concentration of methanol and ethanol, respectively. Due to the benzene volatilization and BaP strict adsorption on the soil mineral and organic fractions, a biocide (kill microorganisms) treatment was added to find out the abiotic loss of benzene and BaP. Biocide treatment preparation has been explained in detail in the supplementary information (SI).

Six treatments, including CK-1 (control-1 with no artificial benzene and BaP added), CK-2 (control-2 with biocide), No-BS (bioremediation with no biostimulant added), BS-ethanol (ethanol as the biostimulant), BS-methanol (methanol as the biostimulant), BS-VO (vegetable oil as the biostimulant), all 6 treatments each triplicate with artificial benzene and BaP added, were set up in the lab. The concentrations of biostimulants were 100 mM ethanol, 100 mM methanol, and 1% vegetable oil (w/w), were selected according to previous studies (Dong et al., 2019; Harkness and Fisher, 2013; Zhao et al., 2019; Zhao et al., 2018). To establish biocide control (CK-2), 2000 mg HgCl₂ kg⁻¹ was added to the selected biocide treatment to inhibit microbial activities (Bianco et al., 2020). In all the treatments, 40% moisture content was retained uniformly, and the bottles were placed at room temperature in darkness to avoid the photodegradation of contaminants. Temperature variations were recorded on a daily basis as shown in (Fig. S1). The benzene and BaP concentrations were analyzed at 1, 2, 4, 8, 16, 28, 40, and 60 days of the incubation period.

2.5. Analytical methods

Butanol-extractable BaP is the bioavailable fraction of BaP for microorganisms to degrade (Duan et al., 2016). Butanol, total extractable BaP (acetone/dichloromethane, 1:1 v/v), and Σ15 PAHs contents were analyzed during the experiment (Umeh et al., 2018). Briefly, 1 g of air-dried soil was extracted thrice with 10 mL of acetone and dichloromethane (1:1 v/v). After ultrasonication, the extracts were dried in a rotary evaporator, followed by the addition of 2 mL of cyclohexane to dissolve the residues. A column of silica gel was prepared and washed with the mixture of n-hexane and dichloromethane (1:1 v/v) solution prior to the addition of the dissolved residues. The eluate was dried under a gentle stream of N₂ and re-dissolved in acetonitrile solution followed by dilution. The solution was filtered through a 2-mL syringe with a 0.22-μm filter membrane. All the butanol, total extractable BaP, and Σ15 PAHs concentrations were measured using the SPD-M20A HPLC system (Shimadzu, Japan) with a fluorescent detector (RF-10AXL) at excitation/emission wavelengths presented by (Huang et al., 2013). To analyze the butanol-extractable fraction, 5 g of soil was mixed with 7.5 mL of butanol, followed by vortex, ultrasonication, and centrifugation (Duan et al., 2016). For the analysis of benzene in soil, 2 g of soil was mixed with 10 mL of n-hexane/acetone (1:1 w/w) solution, followed by vortex for 30 s, ultrasonication for 30 min, centrifugation at 3000 rpm, and filtration through 0.22-mm filter paper. The extract obtained was analyzed through an Agilent gas chromatography-mass spectrometer (GC-MS). The analytical conditions for the determination of BaP, Σ15 PAHs, and benzene contents by HPLC and GC-MS are presented in the supplementary file.

2.6. Enzymatic activities

To further explore the biostimulant-enhanced biodegradation of BaP and benzene co-contaminants, the microbial and enzymatic activities were analyzed in this study. Dehydrogenase (DHA), polyphenol oxidase (PPO), catalase (CAT), and lipase (LPS) activities were measured using the specified kits purchased from Beijing Solarbio Science & Technology Co., Ltd. For the evaluation of DHA activity, 2,3,5-triphenyl tetrazolium chloride was reduced to triphenyl formazone, followed by soil DHA analysis at 485 nm (Sarkar et al., 2010). LPS activity was determined by the hydrolysis of oil ester to fatty acids and the retransformation of fatty acids through the copper soap method, and the final enzyme concentration was analyzed at 710 nm. Soil CAT activity was analyzed by scavenging the peroxide radical at 240 nm. Soil PPO was investigated by the catalysis of pyrogallol into colored substances, and the final product was analyzed at 430 nm using a 96-well micro-quartz plate (Subashchandrabose et al., 2019; Subashchandrabose et al., 2017).

2.7. DNA extraction, quantitative PCR amplification, and illumina high-throughput sequencing

Soil total DNA extraction was accomplished in all samples to classify the microbial diversity in each sample under different treatments. Fast DNA SPIN Kit (MP Biomedicals, USA) was used to extract DNA from each sample according to the manufacturer's instructions. The extracted DNA was verified quantitatively using a NanoDrop ND-2000 spectrophotometer (NanoDrop Technologies, USA) based on spectral absorbance at 260 nm, and its quality was determined using agarose gel electrophoresis. Then, the extracted DNA was dissolved in 80 μL of TE buffer and stored at -20 °C until PCR amplification. The microbial communities were assayed by Illumina MiSeq high-throughput sequencing (Illumina Inc.). The V4 and V5 regions of the bacterial 16S rRNA gene were PCR-amplified using the primers 338F and 806R as described by (Lu et al., 2019). More information about sequencing is presented in the supplementary file.

To quantify the 16S rRNA gene copy number, real-time quantitative PCR (qPCR) was employed to determine the bacterial abundance using the primers 5'-TTCCCGAGTACGAGGGATAC and 5'-TCACGTTGAT-GAACGACAAA (Wang et al., 2018). Clones containing the 16S rRNA gene copy numbers were prepared using Peasy-T1 Simple Cloning Kit (TransGen Biotechnology Co., Ltd, China), according to the manufacturer's instructions. The cloned strains were cultured to extract the plasmid DNA. A standard solution was prepared using serial dilution (10-fold) of the extracted plasmid DNA. The reaction mixture comprised 20 μL of ChamQTM SYBR Color qPCR Master Mix, 2 μL of template DNA (1–10 ng), and 0.5 μmol of each primer. The conditions for the qPCR were as follows: initial denaturation at 95 °C for 30 s and elongation for 39 cycles at 95 °C for 15 s, 56 °C for 30 s, and 72 °C for 30 s prior to the final plate reading. The amplification efficiency (R² values) for 16S rRNA genes copy number ranged from 0.998 to 0.999. The obtained data were deposited in the national center for biotechnology sequence read archive (NCBI-SRA) with accession number PRJNA850664.

2.8. BaP and benzene degradation efficiency and kinetics evaluation

To explore the relationship between biostimulants and contaminants degradation rate, a zero-order kinetic model was applied to fit the bioremediation data. The biodegradation kinetic model can be given as follows:

$$\frac{dC}{dt} = -k_0 \leftrightarrow C_t = C_0 - k_0 \cdot t$$

where C₀ is the initial concentration of benzene and BaP; C_t is the concentration of BaP and benzene at time t, and k₀ is the zero-order kinetic rate constant. The half-life (t_{1/2}) can be calculated as C₀/2k₀

using zero-order kinetic equations. Moreover, the initial concentration for BaP and benzene was analyzed after the completion of the BaP aging period.

2.9. Statistical analysis

The analysis of the degradation of BaP and benzene under the treatments of different biostimulants was performed through SPSS using one-way and two-way ANOVA with a completely randomized design. The mean differences were measured using ≤ 0.05 probability with the least significant differences. Statistical analysis of the \log_{10} of 16S rRNA gene copy number and diversity indices were analyzed through one-way ANOVA. Two-way ANOVA was used for the biodegradation of benzene, BaP, and enzymatic activities. Spearman correlation analysis was done to compare the dominant microorganisms, enzymatic activities, and biodegradation potential of microorganisms. The top most abundant genera were selected and the correlation including statistical analysis was performed via Origin2021pro software.

3. Results and discussion

3.1. Biodegradation of benzene co-contaminated with BaP

3.1.1. BaP and benzene biodegradation efficiency

Co-contamination of BaP highly reduced the biodegradation of benzene compared to the alone benzene contamination, as shown in

(Fig. S2a). Alternatively, the presence of benzene slightly improved the biodegradation of BaP in comparison to individual BaP contamination (Fig. S2b). After the individual and co-contaminants biodegradation analysis, another microcosm experiment was conducted, in which the co-contaminated soil was subjected to biostimulation and the results revealed that biostimulants significantly enhanced the biodegradation of benzene under BaP co-contamination (Fig. 1a, Table S5). Among the different biostimulant groups, the BS-VO group presented the highest benzene biodegradation efficiency of 54.7% under mixed benzene and BaP contamination. Similarly, methanol and ethanol applications also effectively increased the biodegradation of benzene, with an efficiency of 50.6% and 45.8%, respectively, whereas the lowest benzene biodegradation was recorded in the No-BS group (36.9%). Reduced biodegradation of benzene during the presence of BaP could be due to the hazardous impact of BaP on microorganisms. Biostimulation enhanced the microbial activity and capability to degrade hazardous contaminants (Zhang & Lo, 2015; Zhao et al., 2018). Therefore, the biodegradation of benzene was enhanced during biostimulation even in the presence of BaP. Moreover, about 19% of benzene was lost from the biocide group (CK-2), indicating the abiotic loss of benzene during the incubation period (Fig. 1a). The maximum biodegradation of benzene in the BS-VO group is in line with those reported by (Soares et al., 2010), who illustrated that enhanced natural organic matter in soil effectively reduced the volatilization loss and boosted benzene biodegradation.

Biodegradation of BaP was slightly enhanced during the presence of benzene compared to individual BaP contamination (Fig. S2b). In

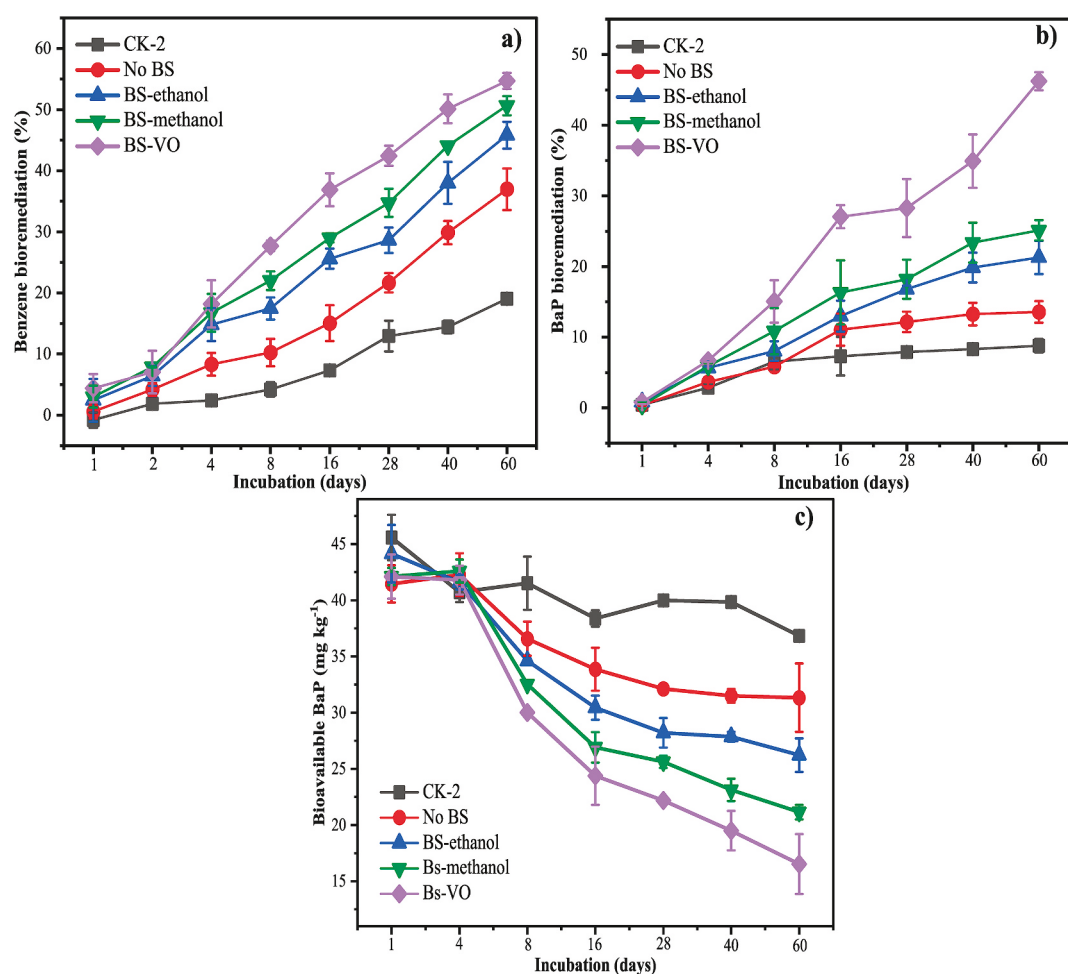


Fig. 1. Biostimulant treatments enhanced biodegradation of a) benzene and b) BaP and c) bioavailable BaP under BaP and benzene co-contamination, where CK-2 represents biocide control, No-BS represents biodegradation with no biostimulant, BS-ethanol represents biodegradation with ethanol, BS-methanol represents biodegradation with methanol, and BS-VO represents biodegradation with vegetable oil.

addition, biostimulation further proliferated the biodegradation of BaP during the co-contaminated conditions (Fig. 1b, Table S6). Among the different treatments, the maximum BaP biodegradation efficiency (46.2%) was observed in the BS-VO group after 60 days of incubation, followed by the BS-methanol group (25.1%), whereas the lowest BaP biodegradation was recorded in the No-BS group (13.6%). The presence of a high amount of dissolved carbon, nitrogen, and other basic nutrients for microbial cell proliferation in vegetable oil (Table S4) might contribute to the efficient biodegradation of BaP co-contaminated with benzene in the BS-VO group. The lowest BaP biodegradation was recorded in the No BS group, which could be due to low microbial and enzymatic activities under the contaminated site, thereby leading to a low biodegradation rate.

The bioavailability constraint of benzene, owing to its high solubility, is less significant when compared with that of BaP (Khoramfar et al., 2020; Wang et al., 2020a); therefore, benzene bioavailability was not discussed in the present study. In contrast, the bioavailability of BaP is a major constraint to its biodegradation, because BaP possesses a strong affinity toward soil minerals and organic matter (Duan et al., 2016; Umeh et al., 2019). Clay-sized particles and hard organic carbon in soil can sequester BaP through physical adsorptions, entrapment, or occlusion in the pores, thus reducing its bioavailability (Taraifdar & Sinha, 2018; Umeh et al., 2019; Wang et al., 2022b). It has been reported that butanol-extractable BaP is the bioavailable fraction of BaP for microbial degradation (Bianco et al., 2020; Umeh et al., 2018; Wang et al., 2020a). In this study, the bioavailability of BaP, quantified as the n-butanol-extractable BaP, decreased with time in all the treatments (Fig. 1c), indicating their degradation or strong adsorption onto soil minerals and organic particles with the passage of time (Duan et al., 2016). Among the different treatment groups, the highest reduction in bioavailable BaP fraction was observed in the BS-VO group, followed by the BS-methanol group, whereas a high level of bioavailable BaP was detected in the CK-2 (biocide) group. The reduction in the bioavailable BaP fraction with time proved that the application of carbonaceous substrates enhanced the biodegradation of bioavailable BaP (Bianco et al., 2020; Li et al., 2021; Meng et al., 2019; Umeh et al., 2019). Correspondingly, Wang et al. (2020a) reported that butanol-extractable BaP fraction could be preferentially degraded by microorganisms when compared with other extractable BaP fractions. Moreover, by comparing biocide and biotic treatments for the bioavailable BaP, a significant difference among the treatments was recorded as shown in (Fig. S3). Therefore, it was concluded that the butanol-extractable BaP fraction was the preferred BaP fraction for biodegradation and that addition of vegetable oil most significantly enhanced the biodegradation of benzene-BaP mixed contaminants in soil.

3.1.2. BaP and benzene biodegradation kinetics

The BaP and benzene biodegradation kinetics (zero order kinetics) were calculated to provide further insight into the biodegradation of benzene and BaP co-contamination under different biostimulant treatments. The biodegradation kinetics parameters, including C_0 , k_0 , $t_{1/2}$, and regression coefficients (R^2), are summarized in Table 1. The degradation rate constant (k_0) for benzene ranged from 0.294 to 0.406 $\text{mg kg}^{-1} \text{ day}^{-1}$, and it is worth noting that the degradation rate of benzene was much lower under the BaP and benzene co-contamination condition when compared with that reported in previous studies. For example, Yang et al. (2019) reported a 15 $\text{mg kg}^{-1} \text{ day}^{-1}$ benzene degradation rate under aerobic conditions under individual benzene contamination. Among the different co-contaminated treatments, the highest benzene degradation rate was noted in the BS-VO group ($k_0 = 0.406 \text{ mg kg}^{-1} \text{ day}^{-1}$) under the co-contamination, followed by the BS-methanol and BS-ethanol groups, whereas the lowest degradation rate ($k_0 = 0.294 \text{ mg kg}^{-1} \text{ day}^{-1}$) was recorded in the No-BS group. Based on these biodegradation rates, the lowest half-life of benzene ($t_{1/2} = 64.2$ days) was recorded in the BS-methanol group, followed by the BS-VO (67.7 days) group, whereas the highest $t_{1/2}$ was observed in the

Table 1

Benzene and BaP biodegradation kinetics under different biostimulant treatments.

| Type of contaminant | Biostimulants | Zero-order kinetics: $C_t = C_0 - k_0 t$ | | | |
|---------------------|---------------|--|--|---------------|-------|
| | | C_0 (mg kg^{-1}) | k_0 ($\text{mg kg}^{-1} \text{ d}^{-1}$) | $t_{1/2}$ (d) | R^2 |
| Benzene | No-BS | 50.9 | 0.294 | 86.6 | 0.966 |
| | BS-ethanol | 50.7 | 0.337 | 75.2 | 0.912 |
| | BS-methanol | 48.0 | 0.374 | 64.2 | 0.893 |
| | BS-VO | 55.0 | 0.406 | 67.7 | 0.826 |
| Benzo[a]pyrene | No-BS | 49.87 | 0.104 | 239.8 | 0.728 |
| | BS-ethanol | 49.76 | 0.164 | 151.7 | 0.859 |
| | BS-methanol | 49.90 | 0.192 | 129.9 | 0.838 |
| | BS-VO | 49.85 | 0.353 | 70.6 | 0.902 |

where No-BS represents biodegradation with no biostimulant, BS-ethanol represents biodegradation with ethanol, BS-methanol represents biodegradation with methanol, and BS-VO represents biodegradation with vegetable oil.

No-BS group. Vegetable oil and methanol can be preferentially used by microorganisms as a carbon source, thus enhancing the biodegradation of benzene under BaP and benzene co-contaminated conditions.

The best fitting for BaP biodegradation was found with the equations of a zero-order kinetic model having regression coefficient (R^2) ranging from 0.728 to 0.902. It has been reported that the biodegradation of low-ring PAHs is best fitted by the first-order kinetics, while that of high-ring PAHs is supported by the zero-order kinetic model (Lu et al., 2012; Yuan and Chang, 2007). Among the biostimulant groups, the BS-VO group showed the highest degradation rate with a k_0 value of 0.353 $\text{mg kg}^{-1} \text{ d}^{-1}$ and the corresponding lowest half-life ($t_{1/2}$) of 70.6 days. Similarly, the k_0 values in BS-methanol and BS-ethanol groups were 0.192 and 0.164 $\text{mg kg}^{-1} \text{ d}^{-1}$, respectively, which were consistent with the k_0 value (0.295–0.459 $\text{mg kg}^{-1} \text{ d}^{-1}$) of the two-compartment first-order kinetic model for surfactant-enhanced BaP biodegradation (Guo & Wen, 2021). Moreover, the lowest k_0 value (0.104 $\text{mg kg}^{-1} \text{ day}^{-1}$) for BaP was recorded in the No-BS group with a corresponding $t_{1/2}$ of 239.8 days, demonstrating that the application of biostimulants efficiently enhanced the biodegradation rates of BaP when compared with the No-BS group under benzene and BaP co-contaminated sites. The $t_{1/2}$ of BaP determined in this study is consistent with those reported by Baltronis et al. (2018) during the biodegradation of BaP-heavy metals mixed contaminants ($t_{1/2} = 112\text{--}144$ days).

3.1.3. Evaluation of total PAHs biodegradation

The biodegradation of total $\Sigma 15$ PAHs (excluding acenaphthylene owing to the HPLC detection constraint) is presented in Table 2. Among different PAHs, acenaphthene, anthracene, and dibenz[a,h]anthracene were completely biodegraded in all the biostimulant-treated groups. The concentrations of some low molecular weight PAHs, such as naphthalene, phenanthrene, pyrene, and chrysene, in different groups, were higher than their initial concentration (Table 2), which can be resulted from the biodegradation of high molecular weight (HMW) PAHs (Madrid et al., 2019). Similarly, Husain (2008) reported an increased pyrene concentration during the biodegradation process of BaP indicating the conversion of BaP into pyrene. Chrysene was completely biodegraded in the CK-1 group, whereas a high amount of chrysene was observed in all the biostimulant groups. Among the different biostimulant groups, the highest amount of chrysene (3.771 mg kg^{-1}) was observed in the BS-VO group, which was owing to the highest biodegradation efficiency of BaP with the biostimulation of vegetable oil, consistent with the observation by Rani and Shanker (2019). Benzo[b]fluoranthene, ranked 10th among the top hazardous contaminants (ATSDR, 2019), was completely biodegraded in the BS-VO group. In contrast, only minor degradation of high molecular weight PAHs, such as benzo[ghi]pyrene, and indeno[1,2,3-cd]pyrene, was observed in different treatment groups, which can be attributed to their high recalcitrance and low bioavailability, making them more resistant to

Table 2Evaluation of total PAHs (mg kg^{-1}) after 60 days of biostimulant-enhanced biodegradation of benzene and BaP co-contaminants.

| PAHs | IC | CK-1 | No BS | BS-ethanol | BS-methanol | BS-VO |
|----------------|---------------|---------------|---------------|---------------|---------------|---------------|
| NAP | 0.167 ± 0.002 | 0.166 ± 0.003 | 0.189 ± 0.031 | 0.167 ± 0.001 | 0.165 ± 0.002 | 0.171 ± 0.002 |
| ACE | 0.069 ± 0.041 | 0.059 ± 0.024 | 0.063 ± 0.014 | ND | ND | ND |
| FLUO | 0.032 ± 0.011 | 0.036 ± 0.008 | 0.014 ± 0.139 | 0.014 ± 0.003 | 0.016 ± 0.003 | 0.029 ± 0.006 |
| PHE | 0.346 ± 0.004 | 0.319 ± 0.027 | 0.348 ± 0.180 | 0.288 ± 0.007 | 0.327 ± 0.024 | 0.342 ± 0.049 |
| ANT | 0.064 ± 0.007 | 0.021 ± 0.017 | 0.054 ± 0.008 | ND | ND | ND |
| FLUA | 0.516 ± 0.066 | 0.474 ± 0.246 | 0.483 ± 0.252 | 0.182 ± 0.014 | 0.248 ± 0.030 | 0.270 ± 0.179 |
| PYR | 0.476 ± 0.049 | 0.345 ± 0.115 | 0.635 ± 0.238 | 0.511 ± 0.024 | 0.497 ± 0.012 | 0.489 ± 0.191 |
| BaA | 0.509 ± 0.053 | 0.233 ± 0.101 | 0.429 ± 0.155 | 0.159 ± 0.026 | 0.205 ± 0.041 | 0.223 ± 0.100 |
| CHR | 0.418 ± 0.000 | ND | 2.697 ± 0.370 | 2.427 ± 0.311 | 2.259 ± 0.351 | 3.771 ± 0.787 |
| BbF | 0.917 ± 0.172 | 0.139 ± 0.012 | 0.775 ± 0.136 | 0.139 ± 0.015 | 0.481 ± 0.177 | ND |
| BkF | 0.285 ± 0.041 | 0.078 ± 0.031 | 0.279 ± 0.041 | 0.074 ± 0.026 | 0.083 ± 0.036 | 0.127 ± 0.064 |
| BaP | 0.450 ± 0.042 | 0.172 ± 0.013 | 43.2* ± 1.53 | 39.4* ± 2.33 | 37.4* ± 1.44 | 26.9* ± 1.27 |
| DB(a,h)A | 0.143 ± 0.037 | ND | ND | ND | ND | ND |
| B(ghi)P | 0.489 ± 0.035 | 0.195 ± 0.025 | 0.440 ± 0.270 | 0.147 ± 0.025 | 0.229 ± 0.016 | 0.269 ± 0.057 |
| In-[1,2,3-cd]P | 0.435 ± 0.021 | 0.215 ± 0.066 | 0.440 ± 0.108 | 0.171 ± 0.013 | 0.211 ± 0.025 | 0.165 ± 0.028 |

where IC represents initial concentration, CK-1 represents control with no contamination, No-BS represents biodegradation with no biostimulant, BS-ethanol represents biodegradation with ethanol, BS-methanol represents biodegradation with methanol, and BS-VO represents biodegradation with vegetable oil. ND = not detected, * = soil was artificially contaminated with 50 mg BaP kg^{-1} soil, NAP = naphthalene, ACE = acenaphthene, Fluo = fluorene, PHE = phenanthrene, ANT = anthracene, FLUA = fluoranthene, PYR = pyrene, BaA = benzo[a]anthracene, CHR = chrysene, BbF = benzo[b]fluoranthene, BkF = benzo[k]fluoranthene, BaP = benzo[a]pyrene, DB(a,h)A = dibenzo[a,h]anthracene, B(ghi)P = benzo[ghi]pyrene, In-[1,2,3-cd]P = indeno[1,2,3-cd]perylene.

biodegradation. These results are in line with the findings of previous studies (Bezza & Chirwa, 2017; Liang et al., 2017; Bianco et al., 2022b) that HMW PAHs were the least degradable owing to their high recalcitrancy.

3.2. Enzymatic activities during biodegradation of benzene-BaP co-contaminants

The soil lipase (LPS), dehydrogenase (DHA), catalase (CAT), and

polyphenol oxidase (PPO) activities were analyzed to obtain further insights into the enhanced biodegradation of BaP-benzene co-contaminants in soil. As shown in (Tables S7–S10), soil LPS, DHA, CAT, and PPO activities were significantly affected by different groups under benzene and BaP co-contamination. Soil LPS activity functions as the hydrolysis of fats and it encompasses the hydrolytic catalysis of oil esters to fatty acids, and can directly reflect the microbial metabolic activities in the soil (Zhou et al., 2020). The maximum LPS activity was recorded in the BS-VO group, followed by the BS-ethanol and BS-methanol groups,

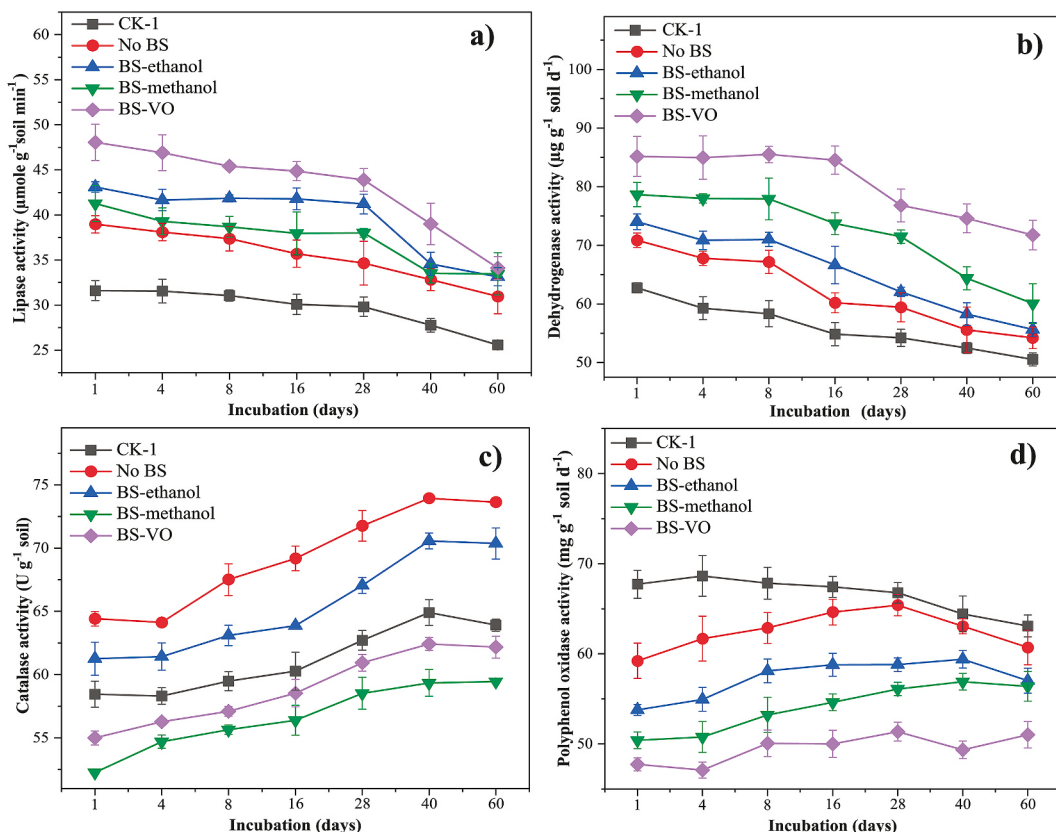


Fig. 2. Activities of soil a) LPS, b) DHA, c) CAT, and d) PPO during biodegradation of BaP-benzene co-contaminants, where CK-1 represents control with no contamination, No-BS represents biodegradation with no biostimulant, BS-ethanol represents biodegradation with ethanol, BS-methanol represents biodegradation with methanol, and BS-VO represents biodegradation with vegetable oil.

whereas the lowest LPS activity was observed in the CK-1 group. High LPS activity is an indicator of high microbial activity under biostimulation, resulting in higher biodegradation of hydrocarbons (Ray et al., 2022). Similarly, Ilesanmi et al. (2020) reported that olive oil acted as the best carbon and nitrogen source to maintain the maximum LPS activity in contaminated soils. The soil LPS activity decreased with time in the biostimulant treatment groups (Fig. 2a), indicating the consumption of added substrates during the 60 days of incubation (Vaithyanathan et al., 2021).

Dehydrogenases (DHA) are enzymes that catalyze reduction reactions through the transfer of hydrogen ions (protons) from the substrate to an acceptor or co-enzyme. Soil DHA activity is an index more relevant to hydrocarbon biodegradation (Liu et al., 2018; Shen et al., 2016). Similar to the trend of LPS activity, the maximum soil DHA activity was noted in the BS-VO group, followed by the BS-methanol group, whereas the lowest DHA activity was recorded in the CK-1 group (Fig. 2b). The high DHA activity in the BS-VO group reflected the strong biodegradation of BaP and benzene co-contamination in the group. It must be noted that DHA activity has a positive correlation with the degradation of aromatic hydrocarbons, and an increase in DHA activity can be elucidated as an indicator of improved microbial degradation of organic contaminants (Bodor et al., 2021; Wu et al., 2017).

Soil catalase (CAT) activity can scavenge peroxide (H_2O_2) produced in soil (Subashchandrabose et al., 2017). The maximum CAT activity was recorded in the No-BS group, followed by the BS-ethanol group, whereas the lowest CAT activities were observed in the BS-methanol and BS-VO groups (Fig. 2c). The decrease in CAT activity was noted in the BS-methanol and BS-VO groups indicated lower production of reactive oxygen species (ROS, H_2O_2) in these groups (Hao et al., 2018). These results are in line with those reported by Subashchandrabose et al.

(2017), who demonstrated that lower CAT activity represented low H_2O_2 (ROS) production. Therefore, the addition of biostimulants such as methanol and vegetable oil significantly reduced the oxidative stress, resulting in high biodegradation of contaminants.

Soil polyphenol oxidase (PPO) activity is strongly related to the biodegradation of phenolic compounds in soil (Shi et al., 2018). The PPO activity was decreased in all the biostimulant-treated groups when compared with that in the CK-1 group. The lowest PPO activity was recorded in the BS-VO group during the 60 days of incubation (Fig. 2d), indicating that the dominant microorganisms contained genes encoding DHA, and not PPO (Liu et al., 2018). Similarly (Zhen et al., 2021), reported that the DHA activity was more reactive to the oxidative degradation of aromatic hydrocarbons when compared with PPO activity, thereby resulting in increased degradation of hydrocarbons. High LPS and DHA activities in the BS-VO group indicated the optimal conditions (e.g., the hydrolysis of fats, proton transfer, and reduced oxidative stress) for BaP and benzene biodegradation. A strong positive correlation among BaP and benzene biodegradation, LPS activity, and DHA activity was observed in the group, whereas, PPO activity was negatively correlated with the biodegradation, depicting that PPO is decreasing with the biodegradation of co-contaminants compare to DHA and LPS. In addition, CAT activity was negatively correlated with DHA and biodegradation of benzene and BaP, and a previous study also reported that CAT tended to have a negative correlation with DHA as CAT indicated soil stress which increased with the elevation of soil pollution level (Wang et al., 2019) (Fig. S4).

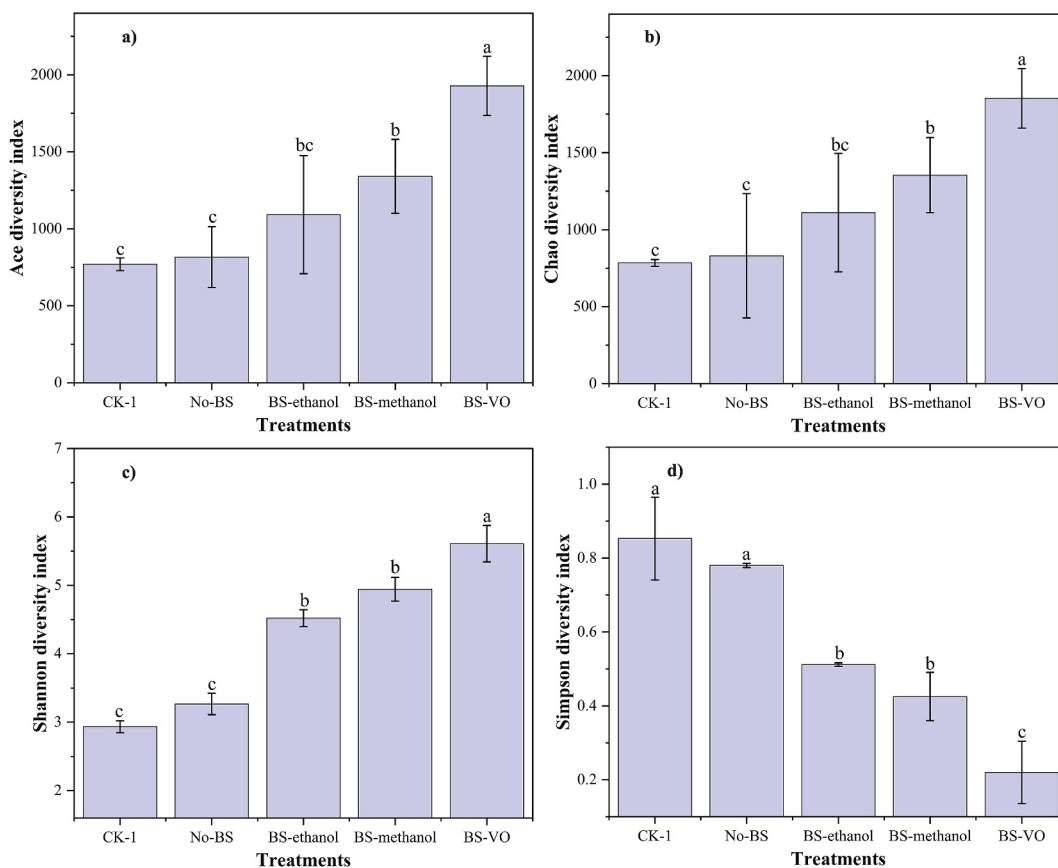


Fig. 3. Microbial diversity indices a) Ace, b) Chao, c) Shannon, and d) Simpson during biodegradation of BaP-benzene co-contaminants, where CK-1 represents control with no contamination, No-BS represents biodegradation with no biostimulant, BS-ethanol represents biodegradation with ethanol, BS-methanol represents biodegradation with methanol, and BS-VO represents biodegradation with vegetable oil.

3.3. Microbial community analysis

3.3.1. Microbial diversity and qPCR

The α -diversity indices, including Ace, Chao, Shannon, and Simpson, were analyzed to evaluate the microbial species richness and evenness in different benzene and BaP co-contaminated conditions (Fig. 3). Chao and Ace diversity indices denote microbial species richness, and their higher values imply a greater variety of microbial species in the sample (Wang et al., 2022a). Ace and Chao diversity indices were the highest in the BS-VO group, followed by BS-methanol, while these indices were lowest in CK-1 and No-BS groups (Fig. 3a, b, c). Carbon-enriched biostimulants are a rich source of energy and can enhance microbial richness and diversity under different contamination conditions (Song et al., 2021; Wu et al., 2020; Wu et al., 2017). Therefore, the rich and readily available carbon in the BS-VO, BS-methanol, and BS-ethanol groups accounted for the increased microbial species richness and diversity. The Shannon and Simpson diversity indices revealed the unevenness within a consortium. It must be noted that the lower Simpson value reflects the more uneven distribution of microbial species (Chen et al., 2021). The Shannon and Simpson indices were significantly different between groups with biostimulants and the No-BS group, suggesting the biostimulants exerted significant influence on the consortium, potentially enriching some genera as discussed further below, hence, resulted in more unevenness in groups with biostimulation. The highest Shannon index and lowest Simpson index were noted in the BS-VO group, indicating that the presence and enriched bacterial consortium played a significant role in the enhanced biodegradation of BaP-benzene co-contaminants.

Furthermore, the β -diversity index was analyzed to observe the microbial community-level differences among the CK-1, No-BS, and different biostimulant-added groups. The results of the PCoA, which was performed on the basis of Euclidian distances among the OTUs at 97% cutoff indicated that PC1 and PC2 accounted for more than 75% of the total variance in the bacterial communities (Fig. 4a). The bacterial communities in the CK-1 group were separated from those in the No-BS group, indicating that the added artificial contaminants altered the microbial consortium significantly. The biostimulant treatment groups are positioned relatively close together after the 60 days of incubation and were separated from the CK-1 and No-BS groups, demonstrating the composite effects of contaminants and biostimulants on the composition and abundance of microbial communities. The presence of readily available carbon sources and the degradation of contaminants causes a substantial change in microbial communities (Huang et al., 2019; Liu et al., 2022; Mosmeri et al., 2019), which can be the rational reason for the differences among the groups with biostimulants, No BS, and CK-1

group.

The qPCR results revealed that co-contamination of benzene and BaP significantly reduced the 16S rRNA gene copy number, indicating that co-contamination poses an adverse effect on microorganisms. However, the biostimulation of benzene and BaP significantly improved the 16S rRNA gene copy number compared to No-BS (Fig. 4b). The gene copy numbers in CK-1 and BS-ethanol were similar, probably due to the composite adverse effect of artificial contaminants and the positive effects of biostimulants. The highest gene copy number was observed in the BS-VO group, showing an increase of 1.4 times the \log_{10} gene copy number when compared with the No-BS group. Biostimulation of soils contaminated with aromatic hydrocarbons has been reported to improve \log_{10} of 16S rRNA gene copies in soil, indicating microbial proliferation under biostimulation (Ahmad et al., 2021; Khudur et al., 2019).

3.3.2. Changes in microbial community composition

Sequences from each treatment group collected after the incubation time were analyzed at both phylum and genus levels to further explore the relationship between the bacterial community structure and their functions (Fig. 5a and b). The primary bacterial phyla (with a relative abundance $>1.0\%$ in all samples) were Proteobacteria, Actinobacteriota, Chloroflexi, Firmicutes, and Acidobacteriota, similar to those observed in previous studies on the biodegradation of individual BaP and benzene contaminants (Lee et al., 2019; Ljesevic et al., 2019; Wang et al., 2020b). Biostimulation of soil under benzene and BaP co-contamination noticeably enhanced the abundance of Proteobacteria, when compared with that in CK-1 and No-BS (Fig. 5a). Among the biostimulant groups, Proteobacteria abundance was at a maximum in the BS-methanol group, followed by BS-VO while the lowest was recorded in the BS-ethanol group. These results reflected that the Proteobacteria abundance increased with the application of biostimulants to BaP and benzene co-contaminated soil, thus making a major contribution to the biodegradation of these co-contaminants. The dominance of Proteobacteria and Actinobacteriota during biostimulation of different contaminated soils could be attributed to their strong contaminants-degrading capabilities (Tejeda-Agredano et al., 2013; Wang et al., 2020b) as well as their ability to completely convert aromatic compounds into CO₂ (Wang et al., 2022a). The dominance of both Proteobacteria and Actinobacteriota in the BS-VO group can be one of the reasons for the high biodegradation of BaP and benzene. These results revealed that Proteobacteria and Actinobacteria need easily degradable substrates for the proliferation and active degradation of contaminants.

Bacterial compositions at the genus level were determined with a relative abundance of more than 5% in all the samples (Fig. 5b).

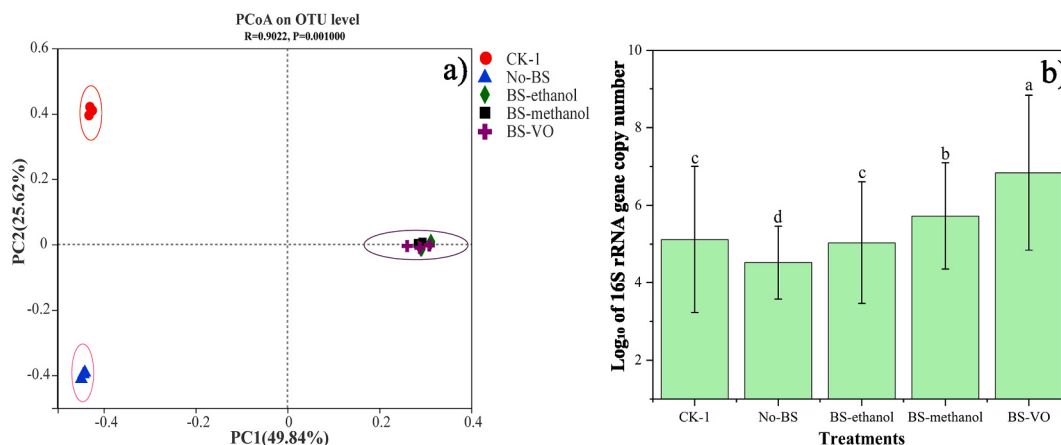


Fig. 4. Microbial community (a) compositions based on the PCoA analysis, and (b) qPCR for the \log_{10} of 16S rRNA gene copy number among different treatments under mixed benzene and BaP co-contamination, where CK-1 represents control with no contamination, No-BS represents biodegradation with no biostimulant, BS-ethanol represents biodegradation with ethanol, BS-methanol represents biodegradation with methanol, and BS-VO represents biodegradation with vegetable oil.

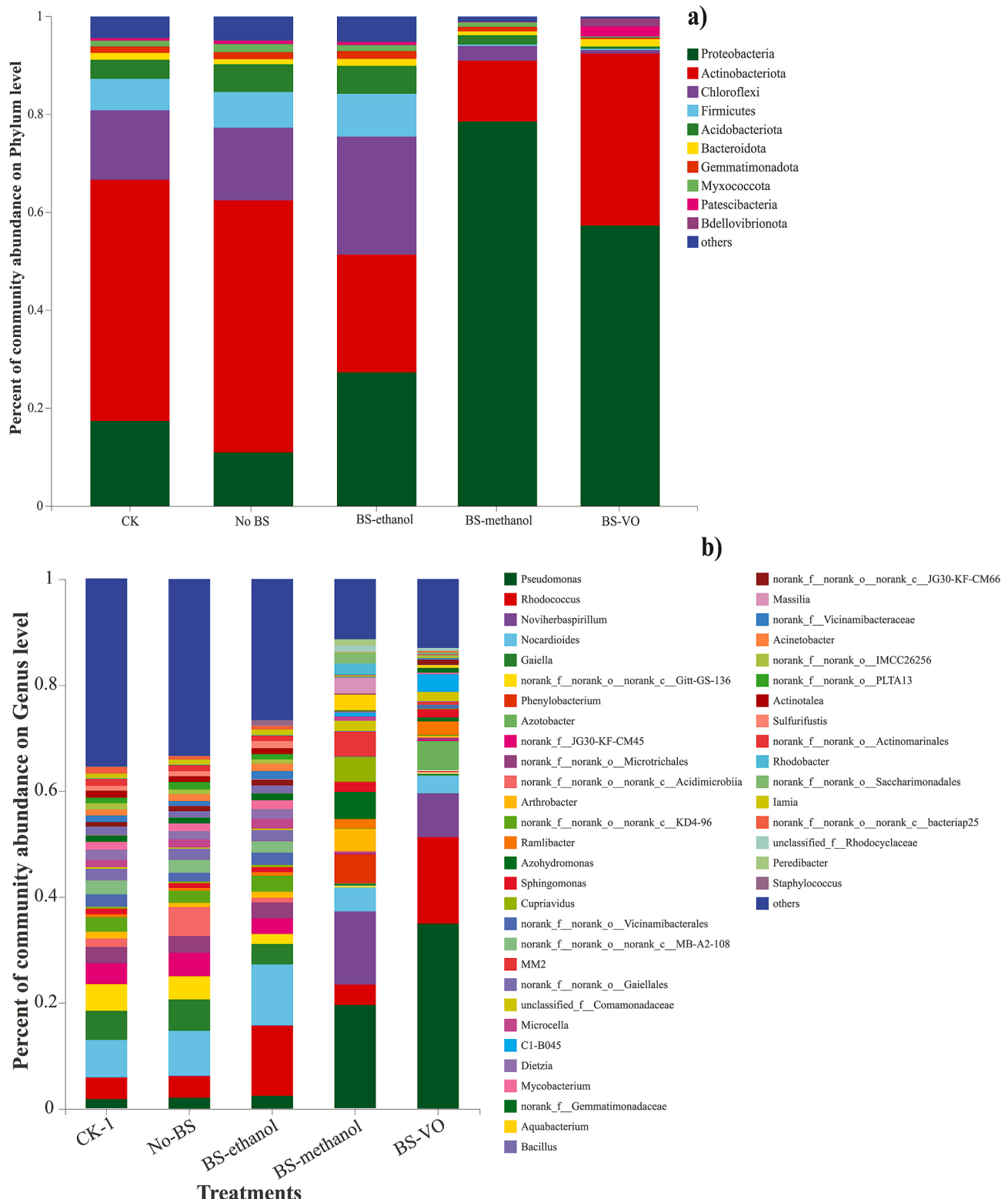


Fig. 5. Bar plot of the microbial community abundance at (a) the phylum level, (b) genus level during biodegradation of BaP-benzene co-contaminants, where CK-1 represents control with no contamination, No-BS represents biodegradation with no biostimulant, BS-ethanol represents biodegradation with ethanol, BS-methanol represents biodegradation with methanol, and BS-VO represents biodegradation with vegetable oil.

Pseudomonas, *Rhodococcus*, *Noviheterospirillum*, *Nocardioides*, and *Gaiella* were the dominant genera after 60 days of incubation time. *Rhodococcus*, *Nocardioides*, and *Gaiella* belong to the phylum Actinobacteriota, capable of degrading large amounts of PAHs and BTEX (Bianco et al., 2021; Chen et al., 2018; Deshpande et al., 2018; Liesevic et al., 2019).

Similarly, *Pseudomonas* and *Noviherbaspirillum* are members of the Proteobacteria phylum with the capacity to degrade high molecular weight PAHs (Wang et al., 2020a). Co-contamination of benzene and BaP (No-BS group) highly reduced the relative abundance of the recognized genera compared to CK-1; however, slight enrichment of the genus

Pseudomonas, *Rhodococcus*, *Noviherbaspirillum*, and *Nocardioides* was recorded with the co-contamination. This enrichment could be associated with their persistence and degrading capabilities under contaminated conditions. In addition, the application of biostimulants noticeably increased the abundance of certain recognized potential genera, when compared with the No-BS group. For example, the application of ethanol enriched *Rhodococcus* and *Nocardioides*; methanol enhanced the abundance of *Pseudomonas* and *Noviherbaspirillum*; whereas vegetable oil proliferated the *Pseudomonas*, *Rhodococcus*, and *Noviherbaspirillum* genera. The variation in abundant microorganisms in different groups indicated competitive growth occurred in the consortium. This can partially explain the enhanced biodegradation efficiency of BaP in the presence of benzene and the reduced biodegradation of benzene in the presence of BaP. In addition, differences among the biostimulant groups indicate the dynamic changes in the substrate depending on bacterial consortium (Fig. 5b). Microbial abundance is highly dependent on the type of substrate added to the contaminated zone, therefore, resulting in their different compositions (Robles et al., 2021; Rangan et al., 2020; Bianco et al., 2022a). For example, Chen et al. (2022) and Umar et al. (2021) reported that *Pseudomonas* has multi-substrate catalytic capabilities to degrade different toxic aromatic compounds completely into CO₂. In addition, *Pseudomonas* and *Rhodococcus* sp. have the potential dehydrogenase genes to degrade toxic aromatic compounds (Ye et al., 2019; Genti-Raimondi et al., 1991). From the results, it was revealed that the enriched functional genera contributed to the increased biodegradation efficiency, however, they responded differently to different biostimulants, resulting in the competitive growth observed in the biostimulant-enhanced groups.

To correlate all the key parameters, including biodegradation rate, enzymes, 16S rRNA (total genes), and dominant bacterial genera, and identify how they collectively play a role in the enhanced biodegradation of BaP and benzene, a Pearson correlation and statistical analysis ($p < 0.05$) were performed (Fig. 6). The analysis revealed that benzene and BaP co-contaminant biodegradation was significantly positively

correlated with the DHA and LPS activities, indicating that these two enzymes are playing an important role in the biodegradation of BaP and benzene co-contaminants. Correspondingly, *Pseudomonas* and *Rhodococcus* genera were positive and significantly correlated with the DHA and LPS activities, indicating that *Pseudomonas* and *Rhodococcus* carried the DHA and LPS-activated genes, capable of biodegrading benzene and BaP co-contamination, which has been reported in previous studies. For example, researchers reported that species of *Pseudomonas* and *Rhodococcus* genera have the potential of encoding genes for DHA, enhancing the catabolic capability of these genera to degrade aromatic hydrocarbons (Kulakov et al., 2000; Li et al., 2011; Medic et al., 2020; Liu et al., 2021). On the other hand, PPO activity was negatively correlated with the biodegradation of benzene and BaP, yet positively correlated with the *Gaiella* and *norank-Gitt-GS-136* genera, suggesting that these genera carried genes for PPO, and could potentially exert a negative influence on the biodegradation of BaP and benzene (Hou et al., 2019; Gabriele et al., 2021).

3.4. Mechanisms of biostimulant-enhanced biodegradation of benzene and BaP

A schematic overview was proposed to describe the enhanced biodegradation mechanisms of benzene and BaP biodegradation (Scheme 1). Two processes have been explained in this schematic diagram, including 1) the biodegradation in individual contamination, and 2) the enhanced biodegradation in co-contaminated soil. During individual contamination, the benzene biodegradation efficiency was high, whereas the biodegradation rate of BaP was slow, implying that abundant microorganisms can quickly degrade benzene compared to BaP. Contrastingly, the biodegradation of benzene was highly reduced with BaP co-contamination, while the biodegradation of BaP slightly increased with benzene co-contamination, indicating that BaP toxicity to microorganisms reduced in the presence of benzene. The biostimulation (different carbon sources) approach was applied to enhance

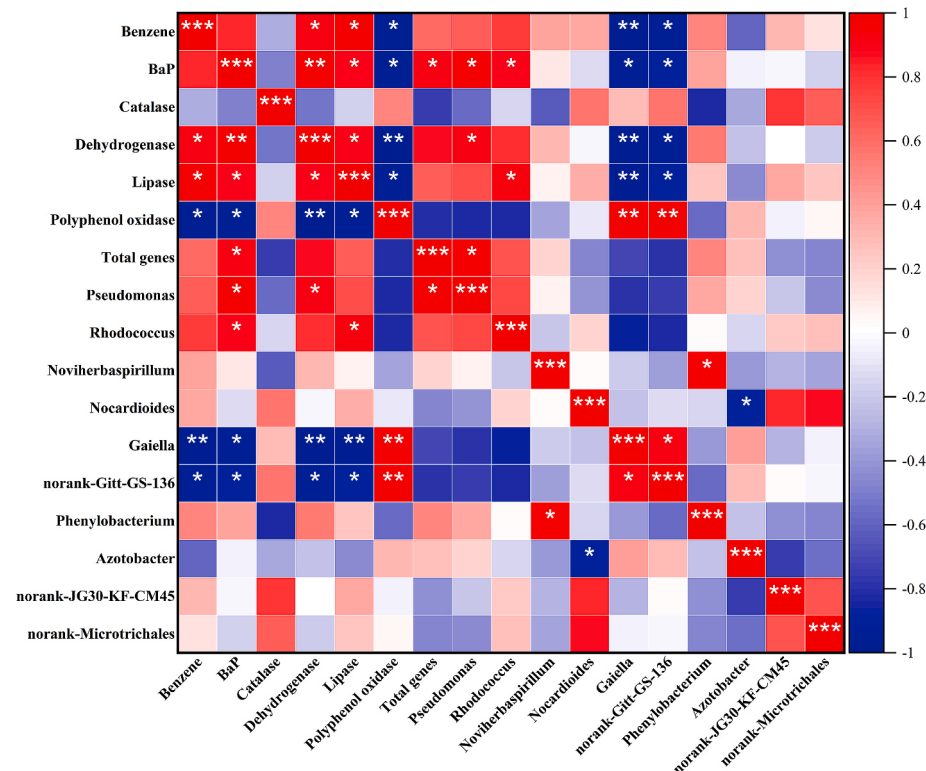
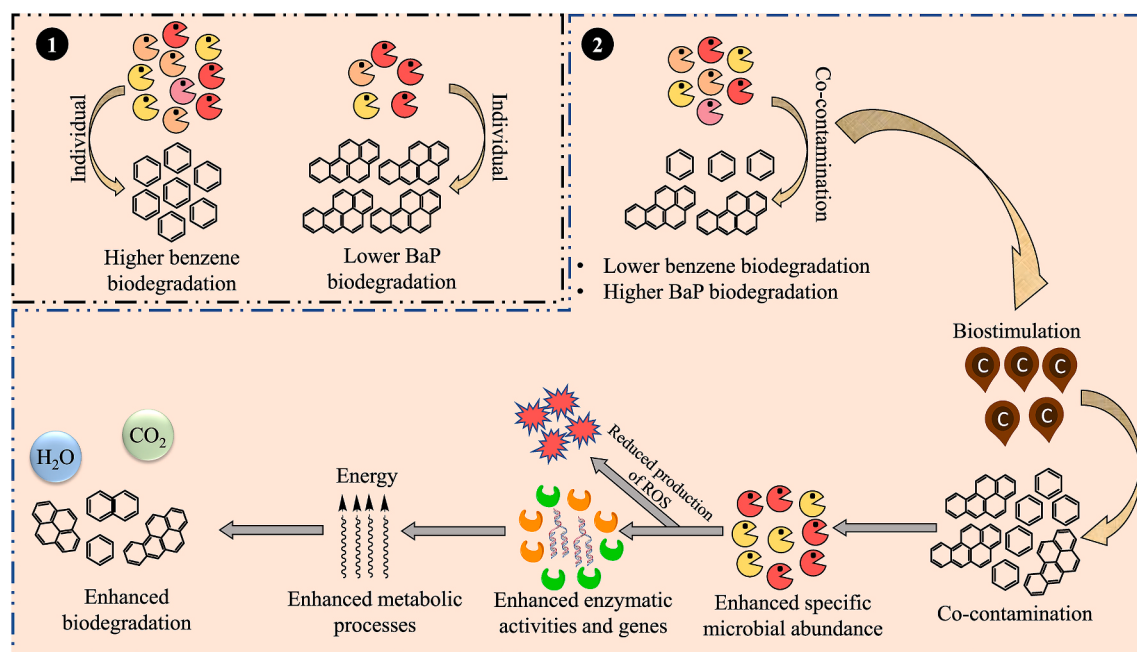


Fig. 6. Pearson correlation with statistical analysis ($*p \leq 0.05$, $**p \leq 0.01$, $***p \leq 0.001$) for the biodegradation of benzene and BaP co-contaminants, enzymes, 16S rRNA (total genes) and top 10 bacterial genera under biostimulant-enhanced biodegradation of BaP and benzene co-contaminated soil.



Scheme 1. Schematic overview of the mechanisms of biostimulant-enhanced biodegradation of benzene and BaP under 1) individual and 2) co-contaminated soils.

the biodegradation of the co-contaminated BaP and benzene soil. The results revealed that the specific microbial diversity was significantly improved during the biostimulation of co-contaminated soil. In addition, the enzymatic activities, including dehydrogenase and lipase were highly enhanced with VO application. Catalase activity, whose function is to scavenge the production of ROS, specifying that the production of ROS can either be reduced with biostimulation or the ROS degrading microorganisms increased with the application of biostimulants.

4. Conclusions

The biostimulation approach for the co-contamination of benzene and BaP was investigated. The results revealed that the biodegradation of BaP increased in the presence of benzene, while the degradation of benzene decreased in the presence of BaP, indicating the potential adverse effect of BaP on benzene-degrading microorganisms. Moreover, the biodegradation of BaP and benzene co-contaminants was significantly enhanced in the biostimulation groups, especially in the BS-VO group, and the bioavailable BaP, which decreased with time, was found to be the preferential fraction of BaP for biodegradation. The enzymatic activities analyzed during the experiment revealed that dehydrogenase and lipase activities were significantly enhanced with the application of biostimulants; whereas, catalase and polyphenol oxidase showed variations among the different treatments. Moreover, the reduction of the enzymatic activities, especially dehydrogenase and lipase were noticed at the end of the incubation, indicating substrate decomposition and the quick detoxification of contaminants. The dominant genera of *Pseudomonas*, *Rhodococcus*, *Noviherbaspirillum*, and *Nocardoides* were enriched upon the biostimulation, indicating their high potential for BaP and benzene co-contaminants biodegradation. The correlation analysis revealed that the biostimulation of vegetable oil significantly improved the abundance of *Pseudomonas* and *Rhodococcus*, capable to encode genes for dehydrogenase, and increased the biodegradation of BaP and benzene. The multiline of evidence for the enhanced biodegradation of co-contaminated BaP and benzene concluded that vegetable oil can be used as a biostimulant for the efficient and safe biodegradation of BaP and benzene co-contaminated soils.

Author contributions

Mukhtiar Ali: Conceptualization, Methodology, Writing-Original Draft; **Xin Song:** Conceptualization, Writing-Review & Editing, Supervision, Project administration; **Qing Wang:** Methodology, Investigation, Data Curation; **Zhuanyia Zhang:** Investigation, Visualization, Data Curation; **Jilu Che:** Investigation, Visualization; **Xing Chen:** Investigation, Data Curation; **Zhiwen Tang:** Investigation; **Xin Liu:** Investigation.

Declaration of competing interest

The authors declare that they have no known competing financial interests or personal relationships that could have appeared to influence the work reported in this paper.

Data availability

Data will be made available on request.

Acknowledgments

This work was supported by the National Key Research and Development Program of China (Grant No. 2019YFC1805700 and No. 2019YFC1805703), the National Natural Science Foundation of China (No. 32061133001), the Major Program of the National Natural Science Foundation of China (No. 41991335), and the CSCEC Environmental Engineering Research Center (Soil Remediation Technology and Equipment) (CSCEC-PT-009).

Appendix A. Supplementary data

Supplementary data to this article can be found online at <https://doi.org/10.1016/j.envpol.2022.120831>.

References

Ahmad, M., Wang, P., Li, J.L., Wang, R., Duan, L., Luo, X., Irfan, M., Peng, Z., Yin, L., Li, W.J., 2021. Impacts of bio-stimulants on pyrene degradation, prokaryotic

- community compositions, and functions. Environ. Pollut. 289, 117863 <https://doi.org/10.1016/j.envpol.2021.117863>.
- Ali, M., Song, X., Ding, D., Wang, Q., Zhang, Z., Tang, Z., 2022. Bioremediation of PAHs and heavy metals co-contaminated soils: challenges and enhancement strategies. Environ. Pollut. 295, 118686 <https://doi.org/10.1016/j.envpol.2021.118686>.
- ATSDR, 2019. Agency for Toxic Substances and Disease Registry US Department of Health and Human Services. Public Health Services, USA.
- Baltrons, O., Lopez-Mesas, M., Vilaseca, M., Gutierrez-Bouzan, C., Le Derf, F., Portet-Koltalo, F., Palet, C., 2018. Influence of a mixture of metals on PAHs biodegradation processes in soils. Sci Total Environ 628-629, 150–158. <https://doi.org/10.1016/j.scitotenv.2018.02.013>.
- Baranger, C., Pezron, I., Lins, L., Deleu, M., Le Goff, A., Fayeulle, A., 2021. A compartmentalized microsystem helps understanding the uptake of benzo[a]pyrene by fungi during soil bioremediation processes. Sci. Total Environ. 784, 147151 <https://doi.org/10.1016/j.scitotenv.2021.147151>.
- Bezza, F.A., Chirwa, E.M.N., 2017. The role of lipopeptide biosurfactant on microbial remediation of aged polycyclic aromatic hydrocarbons (PAHs)-contaminated soil. Chem. Eng. J. 309, 563–576. <https://doi.org/10.1016/j.cej.2016.10.055>.
- Bianco, F., Marciczyk, M., Race, M., Papirio, S., Esposito, G., Oleszczuk, P., 2022a. Low temperature-produced and VFA-coated biochar enhances phenanthrene adsorption and mitigates toxicity in marine sediments. Separ. Purif. Technol. <https://doi.org/10.1016/j.seppur.2022.121414>.
- Bianco, F., Race, M., Papirio, S., Esposito, G., 2020. Removal of polycyclic aromatic hydrocarbons during anaerobic biostimulation of marine sediments. Sci. Total Environ. 709, 136141 <https://doi.org/10.1016/j.scitotenv.2019.136141>.
- Bianco, F., Race, M., Papirio, S., Esposito, G., 2022b. Phenanthrene biodegradation in a fed-batch reactor treating a spent sediment washing solution: techno-economic implications for the recovery of ethanol as extracting agent. Chemosphere 286 (Pt 1), 131361. <https://doi.org/10.1016/j.chemosphere.2021.131361>.
- Bianco, F., Race, M., Papirio, S., Oleszczuk, P., Esposito, G., 2021. The addition of biochar as a sustainable strategy for the remediation of PAH-contaminated sediments. Chemosphere 263, 128274. <https://doi.org/10.1016/j.chemosphere.2020.128274>.
- Bodor, A., Boudjoum, N., Feigl, G., Duzs, A., Laczi, K., Szilagyi, A., Rakheley, G., Perei, K., 2021. Exploitation of extracellular organic matter from *Micrococcus luteus* to enhance ex situ bioremediation of soils polluted with used lubricants. J. Hazard Mater. 417, 125996 <https://doi.org/10.1016/j.jhazmat.2021.125996>.
- Borden, R.C., 2007. Effective distribution of emulsified edible oil for enhanced anaerobic bioremediation. J. Contam. Hydrol. 94 (1–2), 1–12. <https://doi.org/10.1016/j.jconhyd.2007.06.001>.
- Brinch, U.C., Ekelund, F., Jacobsen, C.S., 2002. Method for spiking soil samples with organic compounds. Appl. Environ. Microbiol. 68 (4), 1808–1816.
- Cardenas, E., Wu, W.M., Leigh, M.B., Carley, J., Carroll, S., Gentry, T., Luo, J., Watson, D., Gu, B., Ginder-Vogel, M., Kitaniidis, P.K., Jardine, P.M., Zhou, J., Criddle, C.S., Marsh, T.L., Tiedje, J.M., 2008. Microbial communities in contaminated sediments, associated with bioremediation of uranium to submicromolar levels. Appl. Environ. Microbiol. 74 (12), 3718–3729. <https://doi.org/10.1128/AEM.02308-07>.
- Chen, L., Hu, G., Fan, R., Lv, Y., Dai, Y., Xu, Z., 2018. Association of PAHs and BTEX exposure with lung function and respiratory symptoms among a nonoccupational population near the coal chemical industry in Northern China. Environ. Int. 120, 480–488. <https://doi.org/10.1016/j.envint.2018.08.004>.
- Chen, W., Wang, F., Zeng, L., Li, Q., 2021. Bioremediation of petroleum-contaminated soil by semi-aerobic aged refuse biofilter: optimization and mechanism. J. Clean. Prod. 294 <https://doi.org/10.1016/j.jclepro.2020.125354>.
- Chen, Z., Hu, H., Xu, P., Tang, H., 2022. Soil bioremediation by *Pseudomonas brassicacearum* MPD5 and its enzyme involved in degrading PAHs. Sci. Total Environ. 813, 152522 <https://doi.org/10.1016/j.scitotenv.2021.152522>.
- Deshpande, R.S., Sundaravadivelu, D., Techtmann, S., Conmy, R.N., Santo Domingo, J.W., Campo, P., 2018. Microbial degradation of Cold Lake Blend and Western Canadian select dilbit by freshwater enrichments. J. Hazard Mater. 352, 111–120. <https://doi.org/10.1016/j.jhazmat.2018.03.030>.
- Dobaradaran, S., Schmidt, T.C., Kazuri-Cegla, W., Jochmann, M.A., 2021. BTEX compounds leachates from cigarette butts into water environment: a primary study. Environ. Pollut. 269, 116185 <https://doi.org/10.1016/j.envpol.2020.116185>.
- Dong, J., Yu, D., Li, Y., Li, B., Bao, Q., 2019. Transport and release of electron donors and alkalinity during reductive dechlorination by combined emulsified vegetable oil and colloidal Mg(OH)₂: laboratory sand column and microcosm tests. J. Contam. Hydrol. 225, 103501 <https://doi.org/10.1016/j.jconhyd.2019.103501>.
- Duan, L., Naidu, R., Liu, Y., Dong, Z., Mallavarapu, M., Herde, P., Kuchel, T., Semple, K.T., 2016. Comparison of oral bioavailability of benzo[a]pyrene in soils using rat and swine and the implications for human health risk assessment. Environ. Int. 94, 95–102. <https://doi.org/10.1016/j.envint.2016.04.041>.
- Fu, L., Feng, A., Xiao, J., Wu, Q., Ye, Q., Peng, S., 2021. Remediation of soil contaminated with high levels of hexavalent chromium by combined chemical-microbial reduction and stabilization. J. Hazard Mater. 403, 123847 <https://doi.org/10.1016/j.jhazmat.2020.123847>.
- Gabrielle, I., Race, M., Papirio, S., Esposito, G., 2021. Phytoremediation of pyrene-contaminated soils: a critical review of the key factors affecting the fate of pyrene. J. Environ. Manag. 293, 112805 <https://doi.org/10.1016/j.jenman.2021.112805>.
- Gaga, E.O., Ari, A., Akyol, N., Uzmez, O.O., Kara, M., Chow, J.C., Watson, J.G., Ozel, E., Dogeroglu, T., Odabasi, M., 2018. Determination of real-world emission factors of trace metals, EC, OC, BTEX, and semivolatile organic compounds (PAHs, PCBs and PCNs) in a rural tunnel in Bilecik, Turkey. Sci. Total Environ. 643, 1285–1296. <https://doi.org/10.1016/j.scitotenv.2018.06.227>.
- Genti-Raimondi, S., Marcelo, E.T., Luis, C.P., Alfredo, F., Luis, A.A., 1991. Molecular cloning and expression of the P-hydroxysteroid dehydrogenase gene from *Pseudomonas testosteroni*. Gene 105, 43–49. [https://doi.org/10.1016/0378-1119\(91\)90512-A](https://doi.org/10.1016/0378-1119(91)90512-A).
- Guo, J., Wen, X., 2021. Performance and kinetics of benzo(a)pyrene biodegradation in contaminated water and soil and improvement of soil properties by biosurfactant amendment. Ecotoxicol. Environ. Saf. 207, 111292 <https://doi.org/10.1016/j.ecoenv.2020.111292>.
- Hao, Y., Zhao, L., Sun, Y., Li, X., Weng, L., Xu, H., Li, Y., 2018. Enhancement effect of earthworm (*Eisenia fetida*) on acetylchloride biodegradation in soil and possible mechanisms. Environ. Pollut. 242 (Pt A), 728–737. <https://doi.org/10.1016/j.jenvpol.2018.02.029>.
- Harkness, M., Fisher, A., 2013. Use of emulsified vegetable oil to support bioremediation of TCE DNAPL in soil columns. J. Contam. Hydrol. 151, 16–33. <https://doi.org/10.1016/j.jconhyd.2013.04.002>.
- Hou, L., Liu, R., Li, N., Dai, Y., Yan, J., 2019. Study on the efficiency of phytoremediation of soils heavily polluted with PAHs in petroleum-contaminated sites by microorganism. Environ. Sci. Pollut. Res. Int. 26 (30), 31401–31413. <https://doi.org/10.1007/s11356-019-05828-1>.
- Huang, Y., Pan, H., Wang, Q., Ge, Y., Liu, W., Christie, P., 2019. Enrichment of the soil microbial community in the bioremediation of a petroleum-contaminated soil amended with rice straw or sawdust. Chemosphere 224, 265–271. <https://doi.org/10.1016/j.chemosphere.2019.02.148>.
- Huang, Y., Wei, J., Song, J., Chen, M., Luo, Y., 2013. Determination of low levels of polycyclic aromatic hydrocarbons in soil by high performance liquid chromatography with tandem fluorescence and diode-array detectors. Chemosphere 92 (8), 1010–1016. <https://doi.org/10.1016/j.chemosphere.2013.03.035>.
- Husain, S., 2008. Identification of pyrene-degradation pathways: bench-scale studies using *Pseudomonas fluorescens* 29L. Remed. J. 18 (3), 119–142. <https://doi.org/10.1002/rem.20176>.
- Ilesanmi, O.I., Adekunle, A.E., Omolaiye, J.A., Olorode, E.M., Ogunkanmi, A.L., 2020. Isolation, optimization and molecular characterization of lipase producing bacteria from contaminated soil. Scientific African 8. <https://doi.org/10.1016/j.sciaf.2020.e00279>.
- Kao, C.M., Liao, H.Y., Chien, C.C., Tseng, Y.K., Tang, P., Lin, C.E., Chen, S.C., 2016. The change of microbial community from chlorinated solvent-contaminated groundwater after biostimulation using the metagenome analysis. J. Hazard Mater. 302, 144–150. <https://doi.org/10.1016/j.jhazmat.2015.09.047>.
- Khoramfar, S., Jones, K.D., Ghobadi, J., Taheri, P., 2020. Effect of surfactants at natural and acidic pH on microbial activity and biodegradation of mixture of benzene and xylene. Chemosphere 260, 127471. <https://doi.org/10.1016/j.chemosphere.2020.127471>.
- Khudur, L.S., Shahsavari, E., Webster, G.T., Nugegoda, D., Ball, A.S., 2019. The impact of lead co-contamination on ecotoxicity and the bacterial community during the bioremediation of total petroleum hydrocarbon-contaminated soils. Environ. Pollut. 253, 939–948. <https://doi.org/10.1016/j.envpol.2019.07.107>.
- Kulakov, L.A., Christopher, C.R.A., David, A.L., Michael, J.L., 2000. Cloning and characterization of a novel *cis*-naphthalene dihydrodiol dehydrogenase gene (*narB*) from *Rhodococcus* sp. NCIMB120381. FEMS (Fed. Eur. Microbiol. Soc.) Microbiol. Lett. 182, 327–331.
- Lee, Y., Lee, Y., Jeon, C.O., 2019. Biodegradation of naphthalene, BTEX, and aliphatic hydrocarbons by *Paraburkholderia aromaticivorans* BN5 isolated from petroleum-contaminated soil. Sci. Rep. 9 (1), 860. <https://doi.org/10.1038/s41598-018-36165-x>.
- Li, S., Li, X., Zhao, H., Cai, B., 2011. Physiological role of the novel salicylaldehyde dehydrogenase NahV in mineralization of naphthalene by *Pseudomonas putida* ND6. Microbiol. Res. 166 (8), 643–653.
- Li, X., Luo, T., Wang, Y., Wang, B., Liang, H., Zhou, J., Li, L., 2021. Improving the degradation of benzo[a]pyrene and soil biodegradability by enhanced ozonation with mechanical agitation. Chem. Eng. J. 423 <https://doi.org/10.1016/j.cej.2021.130056>.
- Liang, X., Guo, C., Liao, C., Liu, S., Wick, L.Y., Peng, D., Yi, X., Lu, G., Yin, H., Lin, Z., Dang, Z., 2017. Drivers and applications of integrated clean-up technologies for surfactant-enhanced remediation of environments contaminated with polycyclic aromatic hydrocarbons (PAHs). Environ. Pollut. 225, 129–140. <https://doi.org/10.1016/j.envpol.2017.03.045>.
- Liu, F., Bai, J., Huang, W., Li, F., Ke, W., Zhang, Y., Xie, D., Zhang, B., Guo, X., 2022. Characterization of a novel beta-cypermethrin-degrading strain of *Lactobacillus pentosus* 3-27 and its effects on bioremediation and the bacterial community of contaminated alfalfa silage. J. Hazard Mater. 423 (Pt A), 127101 <https://doi.org/10.1016/j.jhazmat.2021.127101>.
- Liu, Q., Li, Q., Wang, N., Liu, D., Zan, L., Chang, L., Gou, X., Wang, P., 2018. Bioremediation of petroleum-contaminated soil using aged refuse from landfills. Waste Manag. 77, 576–585. <https://doi.org/10.1016/j.wasman.2018.05.010>.
- Liu, X., Ge, W., Zhang, X., Chai, C., Wu, J., Xiang, D., Chen, X., 2019a. Biodegradation of aged polycyclic aromatic hydrocarbons in agricultural soil by *Paracoccus* sp. LXC combined with humic acid and spent mushroom substrate. J. Hazard Mater. 379, 120820 <https://doi.org/10.1016/j.jhazmat.2019.120820>.
- Liu, Y., Gao, P., Su, J., da Silva, E.B., de Oliveira, L.M., Townsend, T., Xiang, P., Ma, L.Q., 2019b. PAHs in urban soils of two Florida cities: background concentrations, distribution, and sources. Chemosphere 214, 220–227. <https://doi.org/10.1016/j.chemosphere.2018.09.119>.
- Liu, Y., Haiyang, H., Giulio, Z., Ping, X., Hongzhi, T., 2021. A *Pseudomonas* sp. strain uniquely degrades PAHs and heterocyclic derivatives via lateral dioxygenation pathways. J. Hazard Mater. 403, 1–10.

- Ljesevic, M., Gojic-Cvijovic, G., Ieda, T., Hashimoto, S., Nakano, T., Bulatovic, S., Illic, M., Beskoski, V., 2019. Biodegradation of the aromatic fraction from petroleum diesel fuel by Oerskovia sp. followed by comprehensive GCxGC-TOF MS. *J. Hazard Mater.* 363, 227–232. <https://doi.org/10.1016/j.jhazmat.2018.10.005>.
- Lominchar, M.A., Lorenzo, D., Romero, A., Santos, A., 2018. Remediation of soil contaminated with PAHs and TPH using alkaline activated persulfate enhanced by surfactant addition at flow conditions. *J. Chem. Technol. Biotechnol.* 93 (5), 1270–1278. <https://doi.org/10.1002/jctb.5485>.
- Lu, C., Hong, Y., Liu, J., Gao, Y., Ma, Z., Yang, B., Ling, W., Waigi, M.G., 2019. A PAH-degrading bacterial community enriched with contaminated agricultural soil and its utility for microbial bioremediation. *Environ. Pollut.* 251, 773–782. <https://doi.org/10.1016/j.envpol.2019.05.044>.
- Lu, X.Y., Li, B., Zhang, T., Fang, H.H., 2012. Enhanced anoxic bioremediation of PAHs-contaminated sediment. *Bioresour Technol* 104, 51–58. <https://doi.org/10.1016/j.biortech.2011.10.011>.
- Madrid, F., Rubio-Bellido, M., Villaverde, J., Pena, A., Morillo, E., 2019. Natural and assisted dissipation of polycyclic aromatic hydrocarbons in a long-term co-contaminated soil with creosote and potentially toxic elements. *Sci. Total Environ.* 660, 705–714. <https://doi.org/10.1016/j.scitotenv.2018.12.376>.
- Medic, A., Ljesevic, M., Inui, H., Beskoski, V., Kojic, I., Stojanovic, K., Karadzic, I., 2020. Efficient biodegradation of petroleum n-alkanes and polycyclic aromatic hydrocarbons by polyextremophilic *Pseudomonas aeruginosa* san ai with multidegradative capacity. *RSC Adv.* 10 (24), 14060–14070.
- Meng, L., Li, W., Bao, M., Sun, P., 2019. Effect of surfactants on the solubilization, sorption and biodegradation of benzo (a) pyrene by *Pseudomonas aeruginosa* BT-1. *J. Taiwan Inst. Chem. Eng.* 96, 121–130. <https://doi.org/10.1016/j.jtice.2019.01.007>.
- Mosmeri, H., Gholami, F., Shavandi, M., Dastgheib, S.M.M., Alaie, E., 2019. Bioremediation of benzene-contaminated groundwater by calcium peroxide (CaO₂) nanoparticles: continuous-flow and biodiversity studies. *J. Hazard Mater.* 371, 183–190. <https://doi.org/10.1016/j.jhazmat.2019.02.071>.
- Muller, J.B., Ramos, D.T., Larose, C., Fernandes, M., Lazzarin, H.S., Vogel, T.M., Corseuil, H.X., 2017. Combined iron and sulfate reduction biostimulation as a novel approach to enhance BTEX and PAH source-zone biodegradation in biodiesel blend-contaminated groundwater. *J. Hazard Mater.* 326, 229–236. <https://doi.org/10.1016/j.jhazmat.2016.12.005>.
- Muller, K., Hubner, D., Huppertsberg, S., Knepper, T.P., Zahn, D., 2022. Probing the chemical complexity of tires: identification of potential tire-borne water contaminants with high-resolution mass spectrometry. *Sci. Total Environ.* 802, 149799.
- Nicholson, C.A., Fathepure, B.Z., 2004. Biodegradation of benzene by halophilic and halotolerant bacteria under aerobic conditions. *Appl. Environ. Microbiol.* 70 (2), 1222–1225.
- Olivito, F., Algieri, V., Jiritano, A., Tallarida, M.A., Tursi, A., Costanzo, P., Maiuolo, L., De Nino, A., 2021. Cellulose citrate: a convenient and reusable bio-adsorbent for effective removal of methylene blue dye from artificially contaminated water. *RSC Adv.* 11 (54), 34309–34318.
- Paneque, P., Caballero, P., Parrado, J., Gomez, I., Tejada, M., 2020. Use of a biostimulant obtained from okara in the bioremediation of a soil polluted by used motor car oil. *J. Hazard Mater.* 389, 121820. <https://doi.org/10.1016/j.jhazmat.2019.121820>.
- Perini, B.L.B., Bitencourt, R.L., Daronch, N.A., dos Santos Schneider, A.L., de Oliveira, D., 2020. Surfactant-enhanced in-situ enzymatic oxidation: a bioremediation strategy for oxidation of polycyclic aromatic hydrocarbons in contaminated soils and aquifers. *J. Environ. Chem. Eng.* 8 (4) <https://doi.org/10.1016/j.jece.2020.104013>.
- Pfeiffer, P., Bielefeldt, A.R., Illangasekare, T., Henry, B., 2005. Partitioning of dissolved chlorinated ethenes into vegetable oil. *Water Res.* 39 (18), 4521–4527. <https://doi.org/10.1016/j.watres.2005.09.016>.
- Picariello, E., Baldantoni, D., De Nicola, F., 2020. Acute effects of PAH contamination on microbial community of different forest soils. *Environ. Pollut.* 262, 114378. <https://doi.org/10.1016/j.envpol.2020.114378>.
- Qin, S., Qi, S., Li, X., Fan, Y., Li, H., Mou, X., Zhang, Y., 2020. Magnetic solid-phase extraction as a novel method for the prediction of the bioaccessibility of polycyclic aromatic hydrocarbons. *Sci. Total Environ.* 728, 138789.
- Rangan, S.M., Mouti, A., LaPat-Polasko, L., Lowry, G.V., Krajmalnik-Brown, R., Delgado, A.G., 2020. Synergistic zerovalent iron (Fe(0)) and microbiological trichloroethene and perchlorate reductions are determined by the concentration and speciation of Fe. *Environ. Sci. Technol.* 54 (22), 14422–14431. <https://doi.org/10.1021/acs.est.0c05052>.
- Rani, M., Shanker, U., 2019. Sunlight mediated improved photocatalytic degradation of carcinogenic benz[a]anthracene and benzof[a]pyrene by zinc oxide encapsulated hexacyanoferrate nanocomposite. *J. Photochem. Photobiol. Chem.* 381 <https://doi.org/10.1016/j.jphotochem.2019.111861>.
- Ray, M., Kumar, V., Banerjee, C., 2022. Kinetic modelling, production optimization, functional characterization and phyto-toxicity evaluation of biosurfactant derived from crude oil biodegrading *Pseudomonas* sp. IITISM 19. *J. Environ. Chem. Eng.* 10 (2) <https://doi.org/10.1016/j.jece.2022.107190>.
- Robles, A., Yellowman, T.L., Joshi, S., Mohana Rangan, S., Delgado, A.G., 2021. Microbial chain elongation and subsequent fermentation of elongated carboxylates as H₂-producing processes for sustained reductive dechlorination of chlorinated ethenes. *Environ. Sci. Technol.* 55 (15), 10398–10410. <https://doi.org/10.1021/acs.est.1c01319>.
- Rodriguez-Morgado, B., Gomez, I., Parrado, J., Garcia, C., Hernandez, T., Tejada, M., 2015. Accelerated degradation of PAHs using edaphic biostimulants obtained from sewage sludge and chicken feathers. *J. Hazard Mater.* 300, 235–242. <https://doi.org/10.1016/j.jhazmat.2015.05.045>.
- Russold, S., Schirmer, M., Piepenbrink, M., Schirmer, K., 2006. Modeling the Impact of a Benzene source zone on the transport behavior of PAHs in groundwater. *Environ. Sci. Technol.* 40, 3565–3571. <https://doi.org/10.1021/es052583o>.
- Sarkar, B., Mallavarapu, M., Yunfei, X., Krishnamurti, G.S.R., Ravi, N., 2010. Sorption of quaternary ammonium compounds in soils: Implications to the soil microbial activities. *J. Hazard Mater.* 184, 448–456. <https://doi.org/10.1016/j.jhazmat.2010.08.055>.
- Sharma, P., Kostarelos, K., Lenschow, S., Christensen, A., de Blanc, P.C., 2020. Surfactant flooding makes a comeback: results of a full-scale, field implementation to recover mobilized NAPL. *J. Contam. Hydrol.* 230, 103602. <https://doi.org/10.1016/j.jconhyd.2020.103602>.
- Shen, W., Zhu, N., Cui, J., Wang, H., Dang, Z., Wu, P., Luo, Y., Shi, C., 2016. Ecotoxicity monitoring and bioindicator screening of oil-contaminated soil during bioremediation. *Ecotoxicol. Environ. Saf.* 124, 120–128. <https://doi.org/10.1016/j.ecoenv.2015.10.005>.
- Shi, W., Guo, Y., Ning, G., Li, C., Li, Y., Ren, Y., Zhao, O., Yang, Z., 2018. Remediation of soil polluted with HMW-PAHs by alfalfa or brome in combination with fungi and starch. *J. Hazard Mater.* 360, 115–121. <https://doi.org/10.1016/j.jhazmat.2018.07.076>.
- Soares, A.A., Albergaria, J.T., Domingues, V.F., Alvim-Ferraz Mda, C., Delerue-Matos, C., 2010. Remediation of soils combining soil vapor extraction and bioremediation: benzene. *Chemosphere* 80 (8), 823–828. <https://doi.org/10.1016/j.chemosphere.2010.06.036>.
- Song, X., Wang, Q., Jin, P., Chen, X., Tang, S., Wei, C., Li, K., Ding, X., Tang, Z., Fu, H., 2021. Enhanced biostimulation coupled with a dynamic groundwater recirculation system for Cr(VI) removal from groundwater: a field-scale study. *Sci. Total Environ.* 772, 145495. <https://doi.org/10.1016/j.scitotenv.2021.145495>.
- Subashchandrabose, S.R., Venkateswarlu, K., Naidu, R., Megharaj, M., 2019. Biodegradation of high-molecular weight PAHs by *Rhodococcus wratislaviensis* strain 9: overexpression of amidohydrolase induced by pyrene and BaP. *Sci. Total Environ.* 651 (Pt 1), 813–821. <https://doi.org/10.1016/j.scitotenv.2018.09.192>.
- Subashchandrabose, S.R., Wang, L., Venkateswarlu, K., Naidu, R., Megharaj, M., 2017. Interactive effects of PAHs and heavy metal mixtures on oxidative stress in *Chlorella* sp. MM3 as determined by artificial neural network and genetic algorithm. *Algal Res.* 21, 203–212. <https://doi.org/10.1016/j.algal.2016.11.018>.
- Tarafdar, A., Sinha, A., 2018. Public health risk assessment with bioaccessibility considerations for soil PAHs at oil refinery vicinity areas in India. *Sci. Total Environ.* 616–617, 1477–1484. <https://doi.org/10.1016/j.scitotenv.2017.10.166>.
- Tejeda-Agredano, M.C., Gallego, S., Vila, J., Grifoll, M., Ortega-Calvo, J.J., Cantos, M., 2013. Influence of the sunflower rhizosphere on the biodegradation of PAHs in soil. *Soil Biol. Biochem.* 57, 830–840. <https://doi.org/10.1016/j.soilbio.2012.08.008>.
- Umar, M.F., Rafatullah, M., Abbas, S.Z., Mohamad Ibrahim, M.N., Ismail, N., 2021. Enhanced benzene bioremediation and power generation by double chamber benthic microbial fuel cells fed with sugarcane waste as a substrate. *J. Clean. Prod.* 310 <https://doi.org/10.1016/j.jclepro.2021.127583>.
- Umeh, A.C., Duan, L., Naidu, R., Semple, K.T., 2018. Time-dependent remobilization of nonextractable benzo[a]pyrene residues in contrasting soils: effects of aging, spiked concentration, and soil properties. *Environ. Sci. Technol.* 52 (21), 12295–12305. <https://doi.org/10.1021/acs.est.8b03008>.
- Umeh, A.C., Duan, L., Naidu, R., Semple, K.T., 2019. Extremely small amounts of B[a]P residues remobilised in long-term contaminated soils: a strong case for greater focus on readily available and not total-extractable fractions in risk assessment. *J. Hazard Mater.* 368, 72–80. <https://doi.org/10.1016/j.jhazmat.2019.01.030>.
- Vaithyanathan, V.K., Savary, O., Cabana, H., 2021. Performance evaluation of biocatalytic and biostimulation approaches for the remediation of trace organic contaminants in municipal biosolids. *Waste Manag.* 120, 373–381. <https://doi.org/10.1016/j.wasman.2020.11.046>.
- Wang, C., Li, Y., Hang, T., Zhang, A., Xie, Y., Wu, B., Xu, H., 2019. A novel microbe consortium, nano-visible light photocatalyst and microcapsule system to degrade PAHs. *Chem. Eng. J.* 359, 1065–1074. <https://doi.org/10.1016/j.cej.2018.11.077>.
- Wang, C., Luo, Y., Tan, H., Liu, H., Xu, F., Xu, H., 2020a. Responsiveness change of biochemistry and micro-ecology in alkaline soil under PAHs contamination with or without heavy metal interaction. *Environ. Pollut.* 266 (Pt 3), 115296. <https://doi.org/10.1016/j.envpol.2020.115296>.
- Wang, H., Chen, P., Zhang, S., Jiang, J., Hua, T., Li, F., 2022a. Degradation of pyrene using single-chamber air-cathode microbial fuel cells: electrochemical parameters and bacterial community changes. *Sci. Total Environ.* 804, 150153. <https://doi.org/10.1016/j.scitotenv.2021.150153>.
- Wang, Q., Guo, S., Ali, M., Song, X., Tang, Z., Zhang, Z., Zhang, M., Luo, Y., 2022b. Thermally enhanced bioremediation: A review of the fundamentals and applications in soil and groundwater remediation. *J. Hazard Mater.* 433, 128749. <https://doi.org/10.1016/j.jhazmat.2022.128749>.
- Wang, Q., Hou, J., Yuan, J., Wu, Y., Liu, W., Luo, Y., Christie, P., 2020b. Evaluation of fatty acid derivatives in the remediation of aged PAH-contaminated soil and microbial community and degradation gene response. *Chemosphere* 248, 125983. <https://doi.org/10.1016/j.chemosphere.2020.125983>.
- Wang, B., Teng, Y., Xu, Y., Chen, W., Ren, W., Li, Y., Christie, P., Luo, Y., 2018. Effect of mixed soil microbiomes on pyrene removal and the response of the soil microorganisms. *Sci. Total Environ.* 640–641, 9–17. <https://doi.org/10.1016/j.scitotenv.2018.05.290>.
- Williams, K.S., Khodier, A., 2020. Meeting EU ELV targets: pilot-scale pyrolysis automotive shredder residue investigation of PAHs, PCBs and environmental contaminants in the solid residue products. *Waste Manag.* 105, 233–239. <https://doi.org/10.1016/j.wasman.2020.02.005>.
- Wu, M., Wu, J., Zhang, X., Ye, X., 2019. Effect of bioaugmentation and biostimulation on hydrocarbon degradation and microbial community composition in petroleum-

- contaminated loess soil. Chemosphere 237, 124456. <https://doi.org/10.1016/j.chemosphere.2019.124456>.
- Wu, M., Ye, X., Chen, K., Li, W., Yuan, J., Jiang, X., 2017. Bacterial community shift and hydrocarbon transformation during bioremediation of short-term petroleum-contaminated soil. Environ. Pollut. 223, 657–664. <https://doi.org/10.1016/j.envpol.2017.01.079>.
- Xiong, W., Lu, Z., Peng, J., 2017. Development of an amendment recipe and identification of benzene degraders for anaerobic benzene bioremediation. Water, Air, Soil Pollut. 229 (1) <https://doi.org/10.1007/s11270-017-3663-3>.
- Xiong, W., Mathies, C., Bradshaw, K., Carlson, T., Tang, K., Wang, Y., 2012. Benzene removal by a novel modification of enhanced anaerobic biostimulation. Water Res. 46 (15), 4721–4731. <https://doi.org/10.1016/j.watres.2012.06.036>.
- Yang, C.F., Liu, S.H., Su, Y.M., Chen, Y.R., Lin, C.W., Lin, K.L., 2019. Bioremediation capability evaluation of benzene and sulfolane contaminated groundwater: determination of bioremediation parameters. Sci. Total Environ. 648, 811–818. <https://doi.org/10.1016/j.scitotenv.2018.08.208>.
- Ye, X., Peng, T., Feng, J., Yang, Q., Pratush, A., Xiong, G., Huang, T., Hu, Z., 2019. A novel dehydrogenase 17beta-HSDx from Rhodococcus sp. P14 with potential application in bioremediation of steroids contaminated environment. J. Hazard Mater. 362, 170–177. <https://doi.org/10.1016/j.jhazmat.2018.09.023>.
- Yuan, S.Y., Chang, B.V., 2007. Anaerobic degradation of five polycyclic aromatic hydrocarbons from river sediment in Taiwan. J Environ Sci Health B 42 (1), 63–69. <https://doi.org/10.1080/03601230601020860>.
- Zegzouti, Y., Boutafda, A., Ezzariai, A., El Fels, L., El Hadek, M., Hassani, L.A.I., Hafidi, M., 2020. Bioremediation of landfill leachate by Aspergillus flavus in submerged culture: evaluation of the process efficiency by physicochemical methods and 3D fluorescence spectroscopy. J. Environ. Manag. 255, 109821 <https://doi.org/10.1016/j.jenvman.2019.109821>.
- Zeng, J., Li, Y., Dai, Y., Wu, Y., Lin, X., 2021. Effects of polycyclic aromatic hydrocarbon structure on PAH mineralization and toxicity to soil microorganisms after oxidative bioremediation by laccase. Environ. Pollut. 287, 117581 <https://doi.org/10.1016/j.envpol.2021.117581>.
- Zhang, Z., Lo, I.M., 2015. Biostimulation of petroleum-hydrocarbon-contaminated marine sediment with co-substrate: involved metabolic process and microbial community. Appl. Microbiol. Biotechnol. 99 (13), 5683–5696. <https://doi.org/10.1007/s00253-015-6420-9>.
- Zhao, Y., Bai, Y., Guo, Q., Li, Z., Qi, M., Ma, X., Wang, H., Kong, D., Wang, A., Liang, B., 2019. Bioremediation of contaminated urban river sediment with methanol stimulation: metabolic processes accompanied with microbial community changes. Sci. Total Environ. 653, 649–657. <https://doi.org/10.1016/j.scitotenv.2018.10.396>.
- Zhao, Y., Li, Z., Ma, J., Yun, H., Qi, M., Ma, X., Wang, H., Wang, A., Liang, B., 2018. Enhanced bioelectroremediation of a complexly contaminated river sediment through stimulating electroactive degraders with methanol supply. J. Hazard Mater. 349, 168–176. <https://doi.org/10.1016/j.jhazmat.2018.01.060>.
- Zhen, L., Hu, T., Lv, R., Wu, Y., Chang, F., Jia, F., Gu, J., 2021. Succession of microbial communities and synergistic effects during bioremediation of petroleum hydrocarbon-contaminated soil enhanced by chemical oxidation. J. Hazard Mater. 410, 124869 <https://doi.org/10.1016/j.jhazmat.2020.124869>.
- Zhou, J., Ge, W., Zhang, X., Wu, J., Chen, Q., Ma, D., Chai, C., 2020. Effects of spent mushroom substrate on the dissipation of polycyclic aromatic hydrocarbons in agricultural soil. Chemosphere 259, 127462. <https://doi.org/10.1016/j.chemosphere.2020.127462>.